

Chemical composition of A and F dwarfs members of the Hyades open cluster^{★,★★}

M. Gebran^{1***}, M. Vick^{1,2}, R. Monier³ and L. Fossati^{4,5}

¹ Groupe de Recherche en Astronomie et Astrophysique du Languedoc, UMR 5024, Université Montpellier II, Place Eugène Bataillon, 34095 Montpellier, France.

e-mail: mgebran@am.ub.es

² Département de Physique, Université de Montréal, Montréal, PQ, H3C 3J7

e-mail: mathieu.vick@umontreal.ca

³Laboratoire Universitaire d’Astrophysique de Nice, UMR 6525, Université de Nice - Sophia Antipolis, Parc Valrose, 06108 Nice Cedex 2, France.

e-mail: Richard.Monier@unice.fr

⁴Institut für Astronomie, Universität Wien, Türkenschanzstrasse 17, 1180 Wien, Austria.

e-mail: fossati@astro.univie.ac.at

⁵Department of Physics and Astronomy, Open University, Walton Hall, Milton Keynes MK7 6AA, UK.

e-mail: l.fossati@open.ac.uk

Received ; accepted

ABSTRACT

Aims. Abundances of **15** chemical elements have been derived for 28 F and 16 A stars members of the Hyades open cluster in order to set constraints on self-consistent evolutionary models including radiative and turbulent diffusion.

Methods. A spectral synthesis iterative procedure was applied to derive the abundances from selected high quality lines in high resolution high signal-to-noise spectra obtained with SOPHIE and AURELIE at the Observatoire de Haute Provence.

Results. The abundance patterns found for A and F stars in the Hyades resemble those observed in Coma Berenices and Pleiades clusters. In graphs representing the abundances versus the effective temperature, A stars often display abundances much more scattered around their mean values than the coolest F stars do. Large star-to-star variations are detected in the Hyades A dwarfs in their abundances of C, Na, Sc, Fe, Ni, Sr, Y and Zr, which we interpret as evidence of transport processes competing with radiative diffusion.

In A and Am stars, the abundances of Cr, Ni, Sr, Y and Zr are found to be correlated with that of iron as in the Pleiades and in Coma Berenices. The ratios [C/Fe] and [O/Fe] are found to be anticorrelated with [Fe/H] as in Coma Berenices. All Am stars in the Hyades are deficient in C and O and overabundant in elements heavier than Fe but not all are deficient in calcium and/or scandium. The F stars have solar abundances for almost all elements except for Si.

The overall shape of the abundance pattern of the slow rotator HD30210 cannot be entirely reproduced by models including radiative diffusion and different amounts of turbulent diffusion.

Conclusions. While part of the discrepancies between derived and predicted abundances could be due to non-LTE effects, the inclusion of competing processes such as rotational mixing and/or mass loss seems necessary in order to improve the agreement between the observed and predicted abundance patterns.

Key words. stars: abundances - stars: main sequence - stars: rotation - diffusion - Galaxy: open clusters and associations: individual: Hyades

1. Introduction

Abundance determinations for A and F dwarfs in open clusters and moving groups aim at elucidating the mechanisms of mixing at play in the interiors of these main-sequence stars. This paper is the third in a series addressing the chemical composition of A and F dwarfs in open clusters of different ages. The objectives of this long-term project are twofold: first, we wish to improve our knowledge of the chemical composition of A and F dwarfs, and

secondly we aim to use these determinations to set constraints on particle transport processes in self consistent evolutionary models. The first paper (Gebran et al. 2008, hereafter Paper I) addressed the abundances of several chemical elements for 11 A and 11 F dwarf members of the Coma Berenices open cluster. In the second paper (Gebran & Monier 2008, Paper II), abundances were derived for the same chemical elements for 16 A and 5 F dwarf members of the Pleiades open cluster. In this study, we present a re-analysis of the A and F dwarf abundances in the Hyades open cluster, already addressed by Varenne & Monier (1999) using mono-order spectra on much more limited spectral ranges (three 70 Å wide spectral intervals). The new data we collected are high signal to noise and high resolution échelle spectra stretching over more than 3000 Å which enabled us to synthesize more lines with high quality atomic data (and

Send offprint requests to: M. Gebran

* Tables 5 to 8 are only available in electronic format at the CDS.

** Based on observations at the Observatoire de Haute-Provence (France).

*** Present affiliation: Departament d’Astronomia i Meteorologia, Universitat de Barcelona, c/ Martí i Franquès, 1, 08028 Barcelona, Spain.

more elements) than in Varenne & Monier (1999). In this paper, abundances have been derived for **15 chemical elements (C, O, Na, Mg, Si, Ca, Sc, Ti, Cr, Mn, Fe, Ni, Sr, Y and Zr)** for 28 F and 16 A members of the Hyades cluster.

Open clusters are excellent laboratories to test stellar evolution theory. Indeed stars in open clusters originate from the same interstellar material, and thus have the same initial chemical composition and age. At a distance of \sim 46 pc (van Leeuwen 2007), the Hyades open cluster is the nearest star cluster and also the most analyzed of all clusters. Perryman et al. (1998) compared the observational HR diagram of the Hyades with stellar evolution models and obtained an estimation of the age of this cluster (\sim 625 Myr) using a combination of Hipparcos data with ground-based photometric indexes. Boesgaard & Friel (1990) derived a metallicity for the Hyades slightly above solar ($<[Fe/H]>=0.127\pm0.022$ dex) from their analysis of Fe I lines in 14 F dwarfs. In a study of 40 Hyades G dwarfs, Cayrel de Strobel et al. (1997) also derived a mean metallicity of $<[Fe/H]>=+0.14\pm0.05$ dex. Abundances derived from calibration of Geneva photometry by Grenon (2000) ($<[Fe/H]>=+0.14\pm0.01$) also yield a slightly enhanced metallicity.

Several papers have addressed the chemical composition of A and F dwarfs in the Hyades open cluster. Carbon and iron abundances have been derived for 14 F stars by Friel & Boesgaard (1990) and Boesgaard & Friel (1990). Lithium abundances have been determined for several F, G and K dwarfs by Cayrel et al. (1984), Boesgaard & Tripicco (1986), Boesgaard & Budge (1988) and Thorburn et al. (1993). Garcia Lopez et al. (1993) have derived the oxygen abundances for 26 F dwarfs members of the Hyades cluster. Carbon, oxygen, sodium, magnesium, silicon, calcium, scandium, chromium, iron, nickel, yttrium and barium abundances have been derived for A stars by Takeda & Sadakane (1997), Hui-Bon-Hoa & Alecian (1998), Burkhardt & Coupry (2000) and Varenne & Monier (1999). Most of these studies, at the exception of Varenne & Monier (1999), have focused mainly on the peculiar Am stars, leaving aside the normal A stars. For a given chemical element, large star-to-star variations were found among A stars in several open clusters like the Pleiades (Paper II) and Coma Berenices (Paper I). Varenne & Monier (1999) found significant star-to-star variations in the abundances of O, Na, Ni, Y and Ba for A stars in the Hyades whereas the F dwarfs display much less dispersion. Similarly, star-to-star variations of [Fe/H], [Ni/H] and [Si/H] are larger for the A dwarfs than for the F dwarfs in the Ursa Major group (Monier 2005). This behavior was also observed in earlier works on field A stars (Holweger et al. 1986, Lambert et al. 1986, Lemke 1998, 1990, Hill & Landstreet 1993, Hill 1995, Rentzsch-Holm 1997 and Varenne 1999).

The incentive to reanalyze the chemical composition of A and F dwarfs of the Hyades is justified by the acquisition of higher quality spectra encompassing a much wider spectral range than used in Varenne & Monier (1999). This allowed us to model more lines of higher quality (ie. with more accurate atomic data) for most investigated chemical elements yielding more accurate abundances for several species.

We have also searched for correlations of the abundances of individual elements with that of iron, an issue not addressed in Varenne & Monier (1999). Furthermore, the state of the art of modelling the internal structure and evolution of A dwarfs has improved over the last ten years and we present here compar-

isons of new models to the observed pattern of abundances. The selection of the stars and the data reduction are described in §2. The determination of the fundamental parameters (T_{eff} and $\log g$) and the spectrum synthesis computations are discussed in (§3). As in Papers I and II, the behavior of the abundances of the analysed chemical elements in A and F dwarfs have been investigated in §4 with respect to effective temperature (T_{eff}), projected rotational velocity ($v_{\text{e}} \sin i$) and the iron abundance ($[{\text{Fe}}/{\text{H}}]$). In §5, the found abundance patterns are compared to recent evolutionary models including self consistent treatment of particle transport (Turcotte et al. 1998b; Richer et al. 2000 and Richard et al. 2001). The abundance pattern of the Am star, HD 30210, is modelled in detail using the latest prescriptions in the Montreal code (Richer et al., 2000). Conclusions are gathered in §6.

2. Program stars, observations and data reduction

Our observing sample consists of 28 F and 16 A members of the Hyades cluster brighter than $V=7$ (the same sample selected by Varenne & Monier 1999). At the distance of the Hyades, $V=7$ mag corresponds to the latest F dwarfs (F8-F9). A Hertzsprung–Russell (HR) diagram of the Hyades, shown in Fig.1, was constructed using the effective temperatures we derived in section 3, the V magnitudes retrieved from SIMBAD and appropriate bolometric corrections. We adopted a cluster distance of 46.5 ± 0.3 pc (van Leeuwen 2007), a reddening of 0.010 ± 0.010 mag (WEBDA¹) and the bolometric corrections given by Balona (1994). The uncertainty on the bolometric correction is of the order of 0.07 mag, leading to a typical uncertainty in M_{bol} of about 0.15 mag, corresponding to an uncertainty of about 0.05 dex in $\log L/L_{\odot}$. In the HR diagram of Fig. 1 the Am stars are depicted as filled squares, the normal A stars as filled circles and the F stars as filled triangles, the spectroscopic binaries as open squares. We did not correct the luminosities of the binaries since the contribution to the total flux due to the secondary is not known.

The age of the cluster can be estimated by adjusting isochrones by Marigo et al. (2008), including overshooting and calculated for a metallicity of $Z = 0.025$ dex, which corresponds roughly to the mean of the recent determinations by Perryman et al. (1998), Castellani et al. (2002), Percival et al. (2003), Salaris et al. (2004), Taylor (2006), Holmberg et al. (2007) plus the value given in WEBDA. Fig.1 displays two isochrones: one corresponding to the age given in WEBDA ($\log t = 8.9$ - full line) and our best fit corresponding to a slightly lower age ($\log t = 8.8$ - dashed line), which agrees quite nicely with the determination by Perryman et al. (1998): $t=625\pm50$ Myr. We are inclined to rule out a lower metallicity which would lead to a much lower value of the age (models without overshooting would lead to a much lower age). Following Landstreet et al.(2007), we have also derived M/M_{\odot} , fractional age (fraction of time spent on the Main Sequence noted as τ) and their uncertainties for each star and collected them in online Table 7. In Fig. 1, the star HD 27962 (= 68 Tau) is located at a much higher effective temperature than the other A dwarfs of similar luminosities. Mermilliod (1982) confirmed its membership to the Hyades and proposed that HD 27962 is a blue straggler with the spectral characteristics of an Am star. Abt (1985) assigned a spectral type Am (A2KA3HA5M) to HD 27962.

¹ www.univie.ac.at/webda/

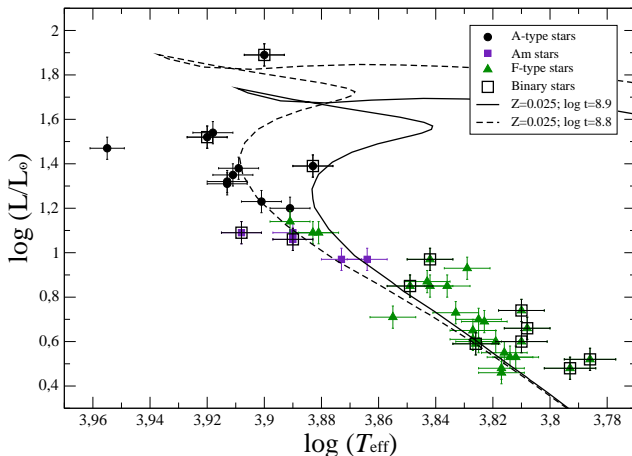


Fig. 1. HR diagram of the Hyades cluster. The two isochrones are calculated with the age given in WEBDA ($\log t=8.9$ - full line) and our best fit ($\log t=8.8$ - dashed line.)

The A stars were observed using SOPHIE, the échelle spectrograph at the Observatoire de Haute-provence (OHP). SOPHIE spectra stretch from 3820 to 6930 Å in 39 orders with two different spectral resolutions: the high resolution mode HR ($R=75000$) and the high efficiency mode HE ($R=39000$). All A stars were observed in the HR mode. The observing dates, exposure times and Signal to Noise ratios achieved for each A star are collected in Table 2. On good nights, an exposure time of 25 minutes typically yielded well exposed spectra with signal-to-noise ratios ranging from 300 to 600, depending on the V magnitude. As we did not get enough observing time to observe the F stars with SOPHIE as well, we have used the mono-order AURELIE spectra obtained by Varenne & Monier (1999). For each F star, three spectral regions centred on $\lambda 6160$ Å, $\lambda 5080$ Å and $\lambda 5530$ Å had been observed at resolutions 30000 ($V \geq 6$) or 60000 ($V \leq 6$) and signal to noise ratios close to 200.

The fundamental data for the selected stars are collected in Table 1. The van Bueren and Henry Draper identifications appear in columns 1 and 2, the spectral type retrieved from SIMBAD or from Abt & Morell (1995) in column 3 and the apparent magnitudes in column 4. Effective temperatures (T_{eff}) and surface gravities ($\log g$), derived from $uvby\beta$ photometry (see section 3), appear in columns 5 and 6. The derived projected rotational velocities and the microturbulent velocities are in columns 7 and 8. Comments about binarity and pulsation appear in the last column. The apparent rotational velocities range from 11 km.s⁻¹ to 165 km.s⁻¹, only 7 stars rotate faster than 100 km.s⁻¹.

Inspection of the CCDM catalogue (Dominican & Nys 1995) reveals that 13 among the 16 A stars are in binary or multiple systems. All of these stars are primaries and the components are much fainter ($1 \text{ mag} < \Delta m < 9.5 \text{ mag}$). Only the case of **HD27962** (CCDM J04255+1755 AB) has to be accounted for because its companion (component B) is three magnitudes fainter than A and at only 1.4'' from A. In case of F stars, 13 among the 28 stars belong to multiple systems. Six of them have nearby companions whose angular distance was probably less than the fiber angular size on the sky (3 arcsec) and who are only three magnitudes fainter than the brightest star we analysed. The spectral types of these companions is unknown. For the F stars, these are:

- **HD26015** = CCDM J04077+1510A has a companion at about 4'' with $\Delta m = 2.8$ mag

- **HD27383** = CCDM J04199+1631AB: components A and B

are very close with $\Delta m = 2.0$ mag

- **HD27991** = CCDM J04257+1557AP: companion P is quoted to be at 0.1'' with $\Delta m = 0.7$ mag

- **HD28363** = CCDM J04290+1610AB is a spectroscopic binary whose angular separation is not specified with a $\Delta m = 1.0$ mag

- **HD30810** = CCDM J04512+1104AB is a triple star whose component B has same magnitude as A, no angular separation is provided.

For these six stars, we believe that the light of the companions might have contaminated the spectra of the brightest components we analysed. The effects are probably most pronounced for the F stars HD26015, HD27383, HD27991, HD28363 and HD30810. The SOPHIE spectra were reduced using IRAF (Image Reduction and Analysis Facility, Tody 1993) in order to properly correct for scattered light. The sequence of IRAF procedures, which follows the method devised by Erspermer & North (2002), is fully described in Paper I.

Table 2. Observing log for the A stars of the Hyades open cluster.

HD	spectral type	exposure time (s)	S/N	Date
27628	A3m	1500	350	10/04/06
27819	A7V	1200	498	10/04/06
27934	A7V	900	591	10/04/06
27962	A2IV	600	429	10/04/06
28226	A3m	1500	380	10/04/06
28319	A7III	300	429	10/04/06
28355	A7V	1500	427	10/04/06
28527	A6IV	1200	354	10/04/06
28546	A5m	1500	292	10/04/06
28910	A8V	1200	434	10/04/06
29388	A6V	600	561	10/05/06
29499	A5m	1320	476	10/05/06
29488	A5V	900	601	10/05/06
30210	Am	1320	474	10/05/06
30780	A7V	1200	549	10/05/06
32301	A7V	720	526	10/05/06

3. Abundance analysis: method and input data

The abundances of 15 chemical elements have been derived by iteratively adjusting synthetic spectra to the normalized spectra and minimizing the chi-square of the models to the observations. Spectrum synthesis is mandatory as the apparent rotational velocities range from 11 to 165 km.s⁻¹. Specifically, synthetic spectra were computed assuming LTE using Takeda's (1995) iterative procedure and double-checked using Hubeny & Lanz (1992) SYNSPEC48 code. This version of SYNSPEC calculates lines for elements up to Z=99.

3.1. Atmospheric parameters and model atmospheres

The effective temperatures and surface gravities were determined using the UVBYBETA code developed by Napiwotzki et al. (1993). This code is based on the Moon & Dworetsky (1985)'s grid, which calibrates the $uvby\beta$ photometry in terms of T_{eff} and $\log g$. The photometric data were taken from Hauck & Mermilliod (1998). The estimated errors on T_{eff} and $\log g$, are ± 125 K and ± 0.20 dex, respectively (see Sec. 4.2 in Napiwotzki et al. 1993). The found effective temperatures and surface gravities are collected in table 1.

Table 1. Basic physical quantities for the programme stars.

vB	HD	Type	m_v	T_{eff} (K)	$\log g$ (cm.s $^{-2}$)	$v_e \sin i$ (km.s $^{-1}$)	ξ_t (km.s $^{-1}$)	Remarks
A stars								
38	27628	A3m	5.72	7310	4.12	31.2	3.70	δ Scuti (d)
47	27819	A7V/A8V	4.80	8190	3.94	47.0	3.00	
54	27934	A7IV/A6V	4.22	8290	3.83	80.0	3.00	
56	27962	A2IV/Am	4.29	9025	3.95	11.3	2.80	Blue Straggler
67	28226	A3m	5.72	7465	4.09	83.0	3.30	
72	28319	A7III/A7IV	3.39	7950	3.70	65.0	2.70	SB (b), δ Scuti (d)
74	28355	A7V/A5m	5.03	7965	3.97	90.0	3.00	
82	28527	A6IV/A7V	4.78	8180	3.98	67.8	3.70	
83	28546	A5m	5.48	7765	4.20	27.5	3.80	SB (b)
95	28910	A8V/A7V	4.65	7640	4.02	110.0	2.60	SB (b), δ Scuti (d)
104	29388	A6V	4.27	8310	3.87	81.0	3.30	SB (b)
107	29499	A5m/A9III	5.39	7770	4.11	60.0	3.00	
108	29488	A5V/A6V	4.70	8150	3.80	118.0	2.60	
112	30210	A2m	5.37	8080	3.92	57.0	4.00	SB (b)
123	30780	A7V/A9V	5.11	7790	3.90	165.0	2.80	δ Scuti (d)
129	32301	A7V	4.64	8110	3.73	117.0	2.70	
F stars								
6	24357	F4V	5.97	6975	4.13	65.5	2.10	
8	25102	F5V	6.37	6685	4.32	64.0	2.20	
11	26015	F3V	6.01	6860	4.46	29.7	1.80	
13	26345	F6V	6.62	6685	4.36	27.2	1.60	
14	26462	F4V	5.73	6945	4.14	18.6	1.50	SB (b)
20	26911	F5V	6.32	6810	4.26	62.1	2.20	
29	27383	F9V	6.88	6215	4.39	16.8	1.40	SB (b)
33	27459	F0V/F0IV	5.26	7785	3.98	73.0	3.10	δ Scuti (d)
35	27524	F5V	6.80	6515	4.24	72.5	2.10	
36	27534	F5V	6.80	6485	4.26	48.0	1.50	
37	27561	F5V	6.61	6710	4.35	22.2	1.60	
51	27848	F8	6.97	6565	4.33	37.7	1.50	
57	27991	F7V	6.46	6430	4.48	17.6	1.10	SB2 (c), SB(b)
75	28363	F8V	6.59	6325	4.43	16.0	1.00	SB3 (c), SB (b)
78	28406	F6V	6.92	6560	4.40	33.0	1.60	
84	28556	F0V	5.41	7635	4.07	83.5	3.30	
85	28568	F2	6.51	6710	4.40	64.0	1.90	
89	28677	F4V/F2V	6.02	7060	4.07	129.0	1.90	SB (b)
90	28736	F5V	6.40	6655	4.30	48.0	1.70	
94	28911	F2	6.62	6590	4.32	50.0	1.60	
100	29169	F5IV	6.02	6950	4.25	75.0	2.20	
101	29225	F8	6.65	6700	4.41	50.8	1.70	SB (b)
111	30034	F0V/A9IV	5.40	7600	4.05	100.0	2.60	
122	30810	F6V	6.76	6110	4.36	12.0	1.10	SB2 (c), SB (b)
124	30869	F5	6.25	6460	4.28	23.5	1.80	SB2 (a,c), SB (b)
126	31236	F3IV/F1V	6.37	7165	3.89	120.0	3.00	
128	31845	F5V	6.75	6550	4.37	33.7	1.90	
154	18404	F5IV	5.80	6740	4.37	26.5	1.70	
	Procyon	F5IV-V	0.34	6650	4.05	6.0	2.2	

References (a) (b) (c) and (d) are for Griffin et al. (1985), Perryman et al. (1998), Barrado & Stauffer (1996) and Solano & Fernley (1997) respectively.

The ATLAS9 (Kurucz 1992) code was used to compute LTE model atmospheres assuming a plane parallel geometry, a gas in hydrostatic and radiative equilibrium and LTE. The ATLAS9 model atmospheres contain 64 layers with a regular increase in $\log \tau_{Ross} = 0.125$ and were calculated assuming Grevesse & Sauval (1998) solar chemical composition. This ATLAS9 version uses the new Opacity Distribution Function (ODF) of Castelli & Kurucz (2003) computed for that solar chemical composition. Convection is calculated in the frame of the mixing length theory (MLT). We have adopted Smalley's prescriptions (Smalley 2004) for the values of the ratios of the

mixing length to the pressure scale height ($\alpha = \frac{L}{H_p}$) and the microturbulent velocities (constant with depth).

3.2. The linelist

For the A stars, the linelist used for spectral synthesis is the same as in Paper I. All transitions between 3000 and 7000 Å from Kurucz's gfall.dat² linelist were selected. The abundance analysis relies on more than 200 transitions for the

² <http://kurucz.harvard.edu/LINELISTS/GFALL/>

15 selected elements as explained in Paper I. The adopted atomic data for each elements are collected in Table 8 of Paper I where, for each element, the wavelength, adopted oscillator strength, its accuracy (when available) and original bibliographical reference are given. The two sodium lines at 5890 and 5896 Å were not used in this present paper. These lines are likely to be affected by **interstellar absorption and** non-LTE effects, an LTE treatment assuming depth independent microturbulence underestimates abundances (Takeda et al. 2009). For the F stars, the same linelist was used except for iron and magnesium since only FeI and MgI lines are available in the AURELIE spectra. We have used the same atomic data for these lines as those in Table 3 of Varenne & Monier (1999). Most of the lines studied here are weak lines formed deep in the atmosphere where LTE should prevail. They are well suited for abundance determinations. **We have also included data for hyperfine splitting for the selected transitions when relevant, using the linelist gfhyperrall.dat³.** However the moderate spectral resolution of the spectra and smearing out of spectra by stellar rotation clearly prevent us from detecting signatures of hyperfine splitting and isotopic shifts in our spectra.

3.3. Spectrum synthesis

For each modelled transition, the abundance was derived iteratively using Takeda's (1995) procedure which minimizes the chi-square between the normalized synthetic spectrum and the observed one. **As explained in Paper I, Takeda's code consists in two routines. The first routine computes the opacity data and it is based on a modified version of Kurucz's Width9 code (Kurucz 1992a) while the second computes the normalized flux and minimizes the dispersion between synthetic and observed spectra (see Paper I for a complete description of the method).**

We first derived the rotational ($v_e \sin i$) and microturbulent (ξ_t) velocities using several weak and moderately strong FeII lines located between 4491.405 Å and 4508.288 Å and the MgII triplet at 4480 Å by allowing small variations around solar abundances of Mg and Fe as explained in Sec. 3.2.1 of Paper I. The weak iron lines are very sensitive to rotational velocity but not to microturbulent velocity while the moderately strong FeII lines are affected mostly by changes of microturbulent velocity. The MgII triplet is sensitive to both ξ_t and $v_e \sin i$. Once the rotational and microturbulent velocities were fixed, we then derived the abundance that minimized the chi-square for each transition of a given chemical element. These individual abundances may differ because of different levels of accuracies in the atomic data of each line and possibly because of deviations from LTE in a few of them. The derivation of the mean abundance from these individual abundances is explained in Sec. 3.5. The abundances were then double-checked using Hubeny & Lanz's (1992) SYNSPEC48 code.

As an example, we display in Fig. 2 the final synthetic spectrum which best fits several Fe II lines in the observed spectrum of HD28527 (A6IV) in the spectral interval 4513–4525 Å. In this region, the independent fit of each line yields only slightly different abundances. The displayed synthetic spectrum is computed for an iron abundance of +0.30 dex, which is the derived mean value in HD28527.

In the case of stars rotating faster than about 80 km/s, the

following neighbouring lines blend: Ti II 4394.059 Å and Ti II 4395.051 Å, Mn I 4033.062 Å and 4034.483 Å and for the O I lines "triplet" at 6155.900 Å, 6156.750 Å and 6158.1 Å. In these cases, the abundances given in the electronic Table 8 are those that provide the best match to each blend.

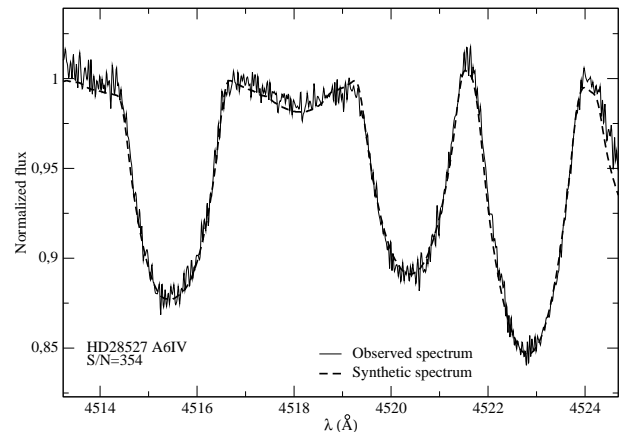


Fig. 2. A typical agreement between the observed spectrum (thin line) of HD28527 (A6IV) and the synthetic spectrum (dashed thick line) computed as explained in Sect. 3. Three iron (FeII) lines calculated for [Fe/H]=+0.30 dex, the mean iron abundance, are displayed in this figure.

3.4. Internal Consistency checks on the spectral energy distribution

For a few stars, we have checked the fundamental parameter determinations by modelling the entire spectral energy distribution from far UV to IR with the theoretical ATLAS9 flux computed for the derived fundamental parameters and the individual abundances. Fig. 3 exemplifies this check for HD 27819. The theoretical spectral energy distribution was computed with the LLmodel code (Shulyak et al. 2004). The observed spectral energy distribution was constructed from Adelman et al's (1989) spectrophotometry and IUE spectrophotometry: SWP04446 (low resolution) + LWP16605 (high resolution resampled to the LWP low resolution). The theoretical LLmodel spectral energy distribution, degraded to a spectral resolution comparable to that of the IUE low resolution spectra, follows nicely the overall shape of the observed flux distribution which leads credence to the adopted fundamental parameters and the derived abundances.

3.5. Mean abundances and uncertainties

Apparent rotational velocity, microturbulent velocity were determined for all sample stars. The abundances of **15** chemical elements were determined for most of the stars (when the selected lines were accessible with good signal-to-noise ratios). The abundances for A and F stars are collected in Online Tables 5 and 6. These abundances are relative to the sun⁴. Solar abundances are from Grevesse & Sauval (1998). **For each chemical element the final abundance is an average of the abundances derived from each line. The errors on the final abundances (labelled**

³ <http://kurucz.harvard.edu/LINELISTS/GFHYPERALL/>

⁴ $[\frac{X}{H}] = \log(\frac{X}{H})_{\star} - \log(\frac{X}{H})_{\odot}$

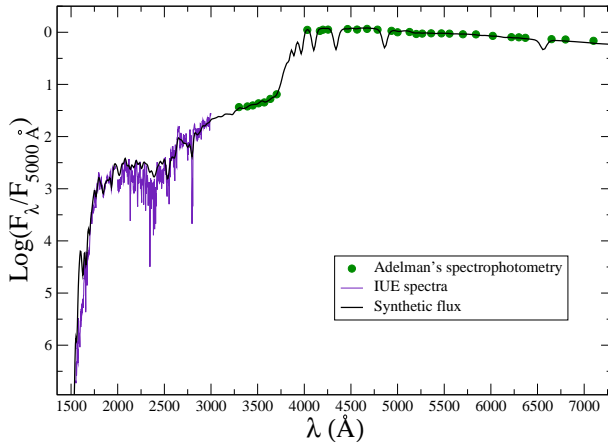


Fig. 3. Comparison of the LLmodel theoretical spectral energy distribution of HD27819 with the observed spectrophotometry of HD 27819 in the UV and the optical.

as σ) are standard deviation assuming a Gaussian distribution of the abundances derived from each line:

$$\bar{x} = \frac{\sum_i x_i}{N} \quad (1)$$

$$\sigma^2 = \frac{\sum_i (x_i - \bar{x})^2}{N} \quad (2)$$

where \bar{x} is the mean value of the abundance, N the number of lines of the element and σ the standard deviation.

Accordingly the error on the abundance of a given element depends on the individual abundances derived from each line and usually varies from star to star. When only one transition was used to derive the abundance (for CI, OI⁵, MgI, SiII, CaII, ScII and YII in F stars), the corresponding error was computed according to the formulation explained in Appendix A of Paper I. It consists into perturbing each of the 6 nominal parameters (T_{eff} , $\log g$, ξ_t , $v_e \sin i$, $\log g f$ and the continuum position) and repeating the fit for each line. The perturbations $\Delta(T_{\text{eff}})$ and $\Delta(\log g)$ are 200 K and 0.20 dex, respectively (Napiwotzki et al. 1993). $\Delta(v_e \sin i)$ is estimated as 5% of the nominal $v_e \sin i$ and $\Delta(\xi_t)$ is 1 km.s⁻¹ (Gebran 2007). $\Delta(\log g f)$ depends on the accuracy of the considered lines. It varies from 3% to more than 50%. For more details concerning the accuracies on the oscillator strengths, see Tab. 8 (3rd column) of Paper I and Tab. 3 (3rd column) of Varenne & Monier (1999). The continuum placement error depends on the rotational velocity of the star and is fully explained in Paper I.

The difference between the nominal abundance and the one derived with the perturbed parameter yields the uncertainty affected to the given parameter. Considering that the errors are independent, the upper limit of the total uncertainty σ_{tot_i} for a given transition (i) is:

$$\sigma_{\text{tot}_i}^2 = \sigma_{T_{\text{eff}}}^2 + \sigma_{\log g}^2 + \sigma_{\xi_t}^2 + \sigma_{v_e \sin i}^2 + \sigma_{\log g f}^2 + \sigma_{\text{cont}}^2. \quad (3)$$

Online Table 8 collects the abundances derived for each transition for each studied element in all A and F stars including Procyon (F5V) which served as control star for

⁵ Oxygen lines are blended in F stars because of the low resolution of AURELIE spectra, which is not the case of SOPHIE's A stars.

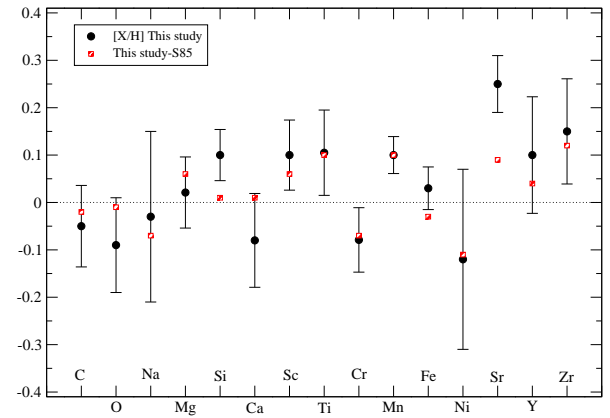


Fig. 4. Comparison of the abundances determined in this study and the one derived by Steffen 1985 (S85) for Procyon (red squares). The derived abundances are in black circles.

the spectral synthesis. In this table, the absolute values are represented ($\log(X/H)_* + 12$) and the wavelengths are in Å.

4. Results

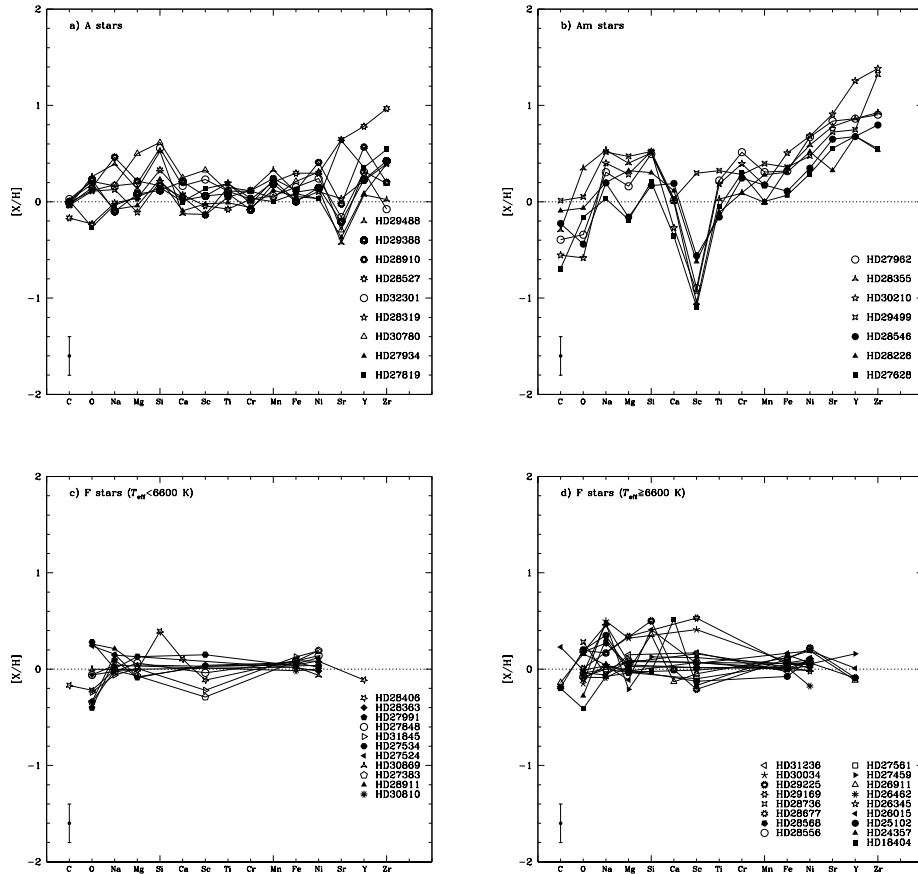
We have first tested the spectrum synthesis on Procyon whose abundances are almost solar (Steffen 1985). For elements having lines on the 3 AURELIE spectral ranges, abundances agree well. The derived abundances are displayed in Fig. 4. We have found nearly solar abundances for all the elements except for strontium. The differences between the abundances we derived and those derived by Steffen (1985) are depicted as squares in Fig. 4. They are less than 0.10 dex for 13 out of 15 elements and less than 0.15 dex for the remaining (Ni and Zr), typically less than the order of magnitude of the uncertainties. We found an apparent rotational velocity of 6 km.s⁻¹ and a microturbulent velocity of 2.2 km.s⁻¹, in good agreement with Steffen's values ($v_e \sin i = 4.5$ km.s⁻¹ and $\xi_t = 2.1$ km.s⁻¹, Steffen 1985).

4.1. Abundance patterns and comparison with previous studies

Abundance patterns graphs where abundances are displayed against atomic number Z are particularly useful to compare the behaviour of A, Am and F stars for different chemical elements. The abundance patterns for A, Am and F stars are displayed in Figs. 5a-d. The pattern for A stars resembles that of the A stars in Coma Berenices and in the Pleiades (Papers I and II). Among the 9 A stars, the elements that exhibit the largest star-to-star variations are Sr, Y and Zr (1.0 to 0.8 dex) while C and Cr display the lowest variations (0.2 dex). The amplitudes of variations for the other elements, O, Na, Mg, Si, Ca, Sc, Ti, Mn, Fe and Ni range from 0.25 to 0.60 dex (see further discussion of individual elements).

The 7 Am stars display the characteristic jig-saw pattern with larger excursions around the solar composition than the A stars do. Almost all Am stars are heavily deficient in Sc, but not all are deficient in Ca and the deficiencies are more modest for this element. Almost all are more deficient in C and O than the A stars, and all are more enriched in iron peak elements and heavy elements (Sr and beyond). For all chemical elements, the star-to-

Fig. 5. Abundance patterns for the "normal" A (a), Am (b) and F (c,d) stars of the Hyades cluster. A maximum ± 0.30 dex error bar is displayed. The horizontal dashed line represents the solar composition.



star variations of Am stars are usually larger than for the A stars. In contrast, F stars exhibit little scatter around the mean abundances. For clarity reasons, the abundances of F stars are sorted out in two graphs: the data for stars cooler than 6600 K appear in Fig. 5c, and for those hotter than 6600 K in Fig. 5d. At the age of the Hyades, a F star with a temperature of 6600 K has a $1.3\text{-}1.4 M_{\odot}$ mass. As explained in sect. 5.1.2, the evolutionary models show that the effects of atomic diffusion are more pronounced in all stars earlier than F5 ($M_{\star} > 1.3 M_{\odot}$) (Turcotte et al. 1998a). Sorting out the F stars into two groups ($T_{\text{eff}} < 6600$ K and $T_{\text{eff}} \geq 6600$ K) helps to highlight the occurrence of diffusion in the most massive F stars.

Graphically, we have compared the abundances derived in this study (filled circles) with previous determinations for 9 stars in Figure 6. The abundances of Mg, Ca, Sc, Cr, Fe and Ni derived by Hui-Bon-Hoa & Alecian (1998) for HD27819, HD27962 and HD30210 are depicted as losanges, the abundances of Si and Fe in HD27819 and HD30210 derived by Burkhardt & Coupry (2000) as empty triangles and those of C, O, Na, Mg, Si, Ca, Sc, Fe, Ni and Y derived by Varenne & Monier (1999) as empty squares. For all stars, the overall shapes of the abundance patterns agree well. Differences exist for individual elements mostly because of the use of different microturbulent velocities, rotational velocities, and in the case of A stars, different ionization levels.

We have also compared the derived iron abundances for F stars

in this work with the compilation available in Perryman et al. (1998) in Table 3. The [Fe/H] determinations come from Chaffee et al. (1971) (CCS), Boesgaard & Budge (1988) (BB), Boesgaard (1989) (B) and Boesgaard & Friel (1990) (BF), they mostly rely on adjustments of theoretical equivalent widths to observed ones. Differences arise from the usage of different effective temperatures with a fixed gravity ($\log g=4.5$ dex), older version of Kurucz ATLAS model atmospheres, different microturbulent velocities (determined using Nissen's 1981 fit) and different neutral iron lines.

4.2. Comments on particular stars

Am stars are expected to be underabundant in light elements, underabundant in calcium and/or scandium as well as overabundant in iron-peak and heavy elements. HD27962 is the hottest A star in the Hyades, Mermilliod (1982) suggested that it may be a blue straggler on basis of its location on the HR diagram. Conti (1965) classified HD 27962 as an Am star based on the weakness of the scandium line at $\lambda 4246$ Å and the strength of strontium line at $\lambda 4215$ Å. Abt (1985) assigned a spectral type Am (A2KA3HA5M) to HD 27962. Our analysis shows that scandium is deficient by -0.90 dex and that iron-peak and heavy elements are enhanced in this star so that it has the characteristics of an Am star. Our analysis of HD28355

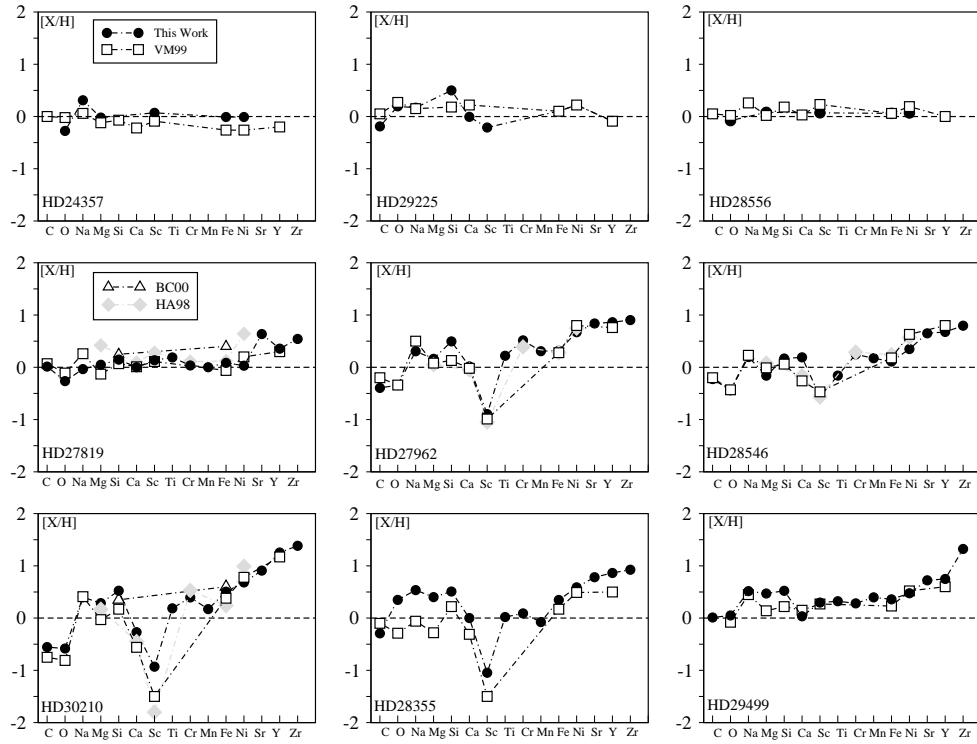


Fig. 6. Comparisons between the abundances derived in this work (filled circles), Varenne & Monier (1999) (VM99, open squares), Hui-Bon-Hoa & Alecian (1998) (HA98, filled diamonds) and Burkhardt & Coupry (2000) (BC00, open triangles) for 9 stars of the Hyades cluster.

(A7V/A5m) also confirms its Am status as scandium is deficient by -1.05 dex and iron-peak and heavy elements are enhanced. Hauck (1977) had previously classified HD28355 as an Am star on basis of Geneva photometry. Both HD 27962 and HD 28355 are classified as Am in the catalog of Renson (1992). The seven stars represented in Fig. 5b are classified as Am in the catalog of Renson (1992). The abundances of all these stars except HD 29499 display the characteristic jig-saw pattern of Am stars: underabundances of light elements, of Ca and/or Sc and overabundances of metals and heavy elements. Our abundance analysis strongly suggest that HD29499 (A5m) may actually be a normal A star: it does not have Ca nor Sc deficiencies and is only moderately enriched in iron-peak and heavy elements. Its apparent rotational velocity is around 60 km.s^{-1} which is rather large for an Am star. Abt & Morrell (1995) have classified HD29499 as a giant star with metallic lines (A9III) but the surface gravity we found for HD 29499 suggests that it still be on the Main Sequence.

4.3. Behavior of the abundances of individual elements

As we have done for the Coma Berenices cluster (see Paper I), the behavior of the found abundances has been studied versus apparent rotational velocity ($v_{\text{e}} \sin i$) and effective temperature (T_{eff}). Any correlation/anticorrelation would be very valuable to theorists investigating the various hydrodynamical mechanisms affecting photospheric abundances. As we emphasized in Paper I, the existence of star-to-star variations with fundamental parameters can be established independently of errors in the absolute values of the oscillator strengths, since all stars will be

Table 3. Iron abundances comparisons.

Star	Reference	[Fe/H]	[Fe/H] _{this work}
HD24357	BB	0.30	-0.014
HD25102	BB	0.20	-0.075
HD26015	BF	0.10	0.166
HD26345	BF	0.18	0.065
HD26462	BF	0.08	0.016
HD26911	BB	0.27	0.120
HD27383	CCS	0.23	0.082
HD27561	BF	0.16	0.048
HD27848	B	0.16	0.086
HD27991	BF	0.11	0.067
HD28406	BF	0.12	0.088
HD28736	BB	0.13	0.009
HD29225	BB	0.19	0.104
HD30810	CCS	0.16	-0.016
HD31845	BF	0.30	0.128

affected in the same manner.

Second, we have searched whether the abundances of individual elements correlate with that of iron. We expect the abundances of Fe, Ti, O, Cr, Mg, Mn, C, Ca and Ni to be fairly reliable as we synthesized several lines of quality A to D for these elements. For Y and Zr, several lines are available but their accuracy is unknown, the abundances of these elements should therefore be taken with caution. The abundances of Sr, derived from 2 transitions whose oscillator strengths

Table 4. Mean abundances and dispersions.

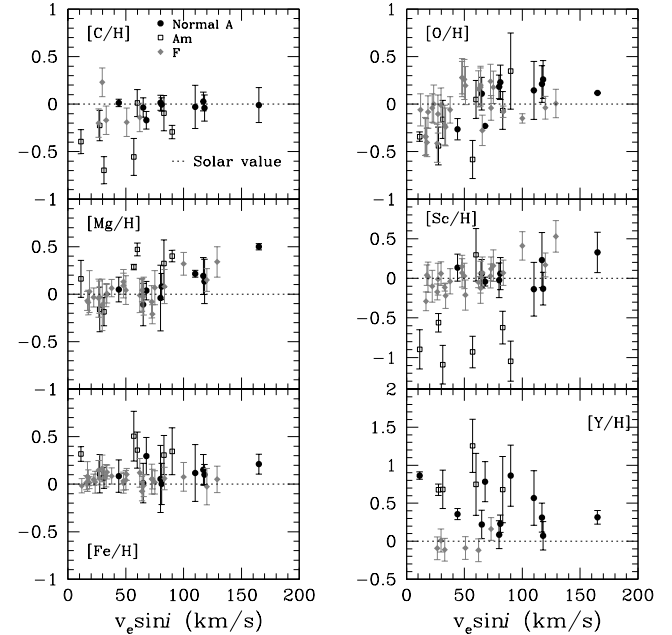
Elements	F stars	σ_F	(Max-Min) $_{[\frac{X}{H}]}$	A stars	σ_A	(Max-Min) $_{[\frac{X}{H}]}$	Am stars	σ_{Am}	(Max-Min) $_{[\frac{X}{H}]}$
$[\frac{C}{H}]$	-0.09	0.16	0.43	-0.15	0.21	0.72	-0.32	0.27	0.71
$[\frac{O}{H}]$	-0.03	0.21	0.69	-0.03	0.27	0.93	-0.17	0.30	0.93
$[\frac{Na}{H}]$	0.11	0.18	0.59	0.20	0.20	0.64	0.31	0.23	0.50
$[\frac{Mg}{H}]$	0.03	0.11	0.55	0.15	0.21	0.68	0.18	0.21	0.66
$[\frac{Si}{H}]$	0.29	0.18	0.52	0.35	0.17	0.50	0.39	0.17	0.36
$[\frac{Ca}{H}]$	0.12	0.24	0.65	0.02	0.16	0.61	-0.04	0.17	0.55
$[\frac{Sc}{H}]$	0.03	0.18	0.82	-0.27	0.49	1.42	-0.69	0.64	1.39
$[\frac{Ti}{H}]$	-	-	-	0.08	0.13	0.48	0.06	0.13	0.48
$[\frac{Cr}{H}]$	-	-	-	0.14	0.16	0.60	0.27	0.21	0.42
$[\frac{Mn}{H}]$	-	-	-	0.17	0.12	0.47	0.18	0.13	0.47
$[\frac{Fe}{H}]$	0.05	0.05	0.24	0.19	0.14	0.50	0.29	0.17	0.44
$[\frac{Ni}{H}]$	0.07	0.09	0.40	0.33	0.21	0.65	0.51	0.26	0.39
$[\frac{Sr}{H}]$	-	-	-	0.29	0.46	1.33	0.68	0.61	0.58
$[\frac{Y}{H}]$	-0.04	0.10	0.28	0.54	0.32	1.18	0.82	0.42	0.57
$[\frac{Zr}{H}]$	-	-	-	0.60	0.41	1.46	0.93	0.53	0.83

have unknown inaccuracies, are likely to be inaccurate.

Abundances are displayed against T_{eff} in the left part of Figs. 8 to 12. Inspection of these figures reveal that there is no systematic slope (positive nor negative) and that for a large number of chemical elements, A stars display star-to-star variations in abundances larger than the typical uncertainty. Table 4 presents the mean abundance, the standard deviation and maximum spread for all chemical elements in **F, A (normal and Am) and Am stars**. Scatter around the mean value is more important in A stars than in F stars, namely for C, Na, Sc, Fe, Ni, Sr, Y and Zr. This behavior was already found in Coma Berenices and the Pleiades (see Papers I and II).

The abundances of C, O, Mg, Sc, Fe and Y are displayed versus $v_e \sin i$ for A, Am and F stars in Fig. 7. For a given element, there is usually a considerable scatter in abundances at a given rotation rate. None of the derived abundances in this study exhibits a clear correlation nor anticorrelation with $v_e \sin i$. Charbonneau & Michaud (1991) have analyzed the effect of meridional circulation on the chemical separation of elements in rotating stars. They showed that for stars rotating at less than $v_e \sin i \leq 100 \text{ km.s}^{-1}$, no correlation should be expected between abundances and apparent rotational velocities. This prediction is verified by our findings (see Fig. 7). Even if we distinguish two velocity regimes ($v_e \sin i \leq 100 \text{ km.s}^{-1}$ and $v_e \sin i \geq 100 \text{ km.s}^{-1}$), we fail to find any dependence between the abundances of any of the 15 chemical elements and the apparent rotational velocity. Recently, Takeda et al. (2008) have found that the peculiarities (underabundances of C, O, and Ca) seen in slow rotators efficiently decrease with an increase of rotation and almost disappear at $v_e \sin i \geq 100 \text{ km.s}^{-1}$. We confirm that for these chemical elements abundance anomalies vanish at $v_e \sin i \geq 100 \text{ km.s}^{-1}$.

Carbon and oxygen abundances display large star-to-star variation in A stars. No clear correlation was found between the abundances of C or O and [Fe/H]. However, both [C/Fe] and [O/Fe] are anticorrelated with [Fe/H]. For the carbon lines used in our study, non-LTE abundance corrections for the A stars ($7000 \text{ K} < T_{\text{eff}} < 10000 \text{ K}$) are expected to be negative (Rentzsch-Holm 1996) and do not affect the

**Fig. 7.** Abundances of C, O, Mg, Sc, Fe and Y versus $v_e \sin i$ for A, Am and F stars.

star-to-star dispersion in [C/H]. Non-LTE corrections for oxygen abundances are negligible in the case of the OI lines considered here (see Paper I). Carbon and Oxygen tend to be more deficient in Am stars than in A stars of similar effective temperatures or rotation rate.

For A stars, sodium abundances appear to be slightly correlated to the iron abundances as seen in Fig. 8. We found important star-to-star abundance variations in $[\text{Na}/\text{H}]$. In Fig. 9, the scatter of $[\text{Mg}/\text{H}]$ for both F and A stars does not exceed the typical uncertainty (0.20 dex) which suggests that there are no significant star-to-star variations in magnesium abundances. As mentioned in Paper I, the MgII $\lambda 4481 \text{ \AA}$

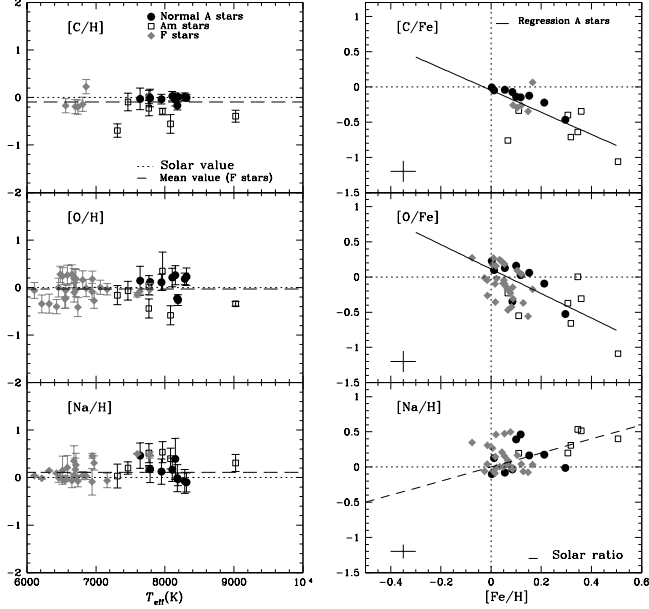


Fig. 8. Left panel: Abundances of carbon, oxygen and sodium versus effective temperature. The dotted line corresponds to the solar value and the dashed line to the mean value determined for the F stars of the cluster. Right panel: [C/Fe], [O/Fe] and [Na/H] versus [Fe/H]. The filled dots correspond to normal A stars, the open squares correspond to Am stars and the filled diamonds correspond to F stars. In the plot representing [Na/H] versus [Fe/H], the dashed line corresponds to the solar [Na/Fe] ratio. The error bars in the right panel represent the mean standard deviation for the displayed abundances.

triplet yields higher abundances than other MgII lines, therefore we excluded this line from our analysis. The corrected [Mg/H] abundances appear to be slightly correlated with [Fe/H]. The ratio [Mg/Fe] is close to solar for the A stars. The silicon lines synthesized in this work have low quality oscillator strengths and have not been updated for the recent values of the log gf of the NIST⁶ database. The systematic found overabundances could be due to incorrect oscillator strengths, therefore the Si abundances should be viewed with caution. There does not seem to be significant star-to-star variations in [Si/H].

Calcium abundance does not exhibit real star-to-star variations neither any clear correlation with respect to [Fe/H]. Not all Am stars are underabundant in calcium, only two of the 7 Am stars exhibit large underabundances in Ca. This result differs from Varenne & Monier's (1999) findings because of the use of different microturbulent velocities and ionisation level as explained in Sec.4.1. In Varenne & Monier (1999), the derived microturbulent abundances were larger (up to 5 km.s⁻¹) than those derived here, leading to lower abundances of calcium. Star-to-star variations in scandium abundance are clearly present for A stars (Fig. 10). Scandium is the most scattered of all analyzed elements. Scandium abundances do not appear to be correlated to iron abundances for both A and F stars. All Am stars except

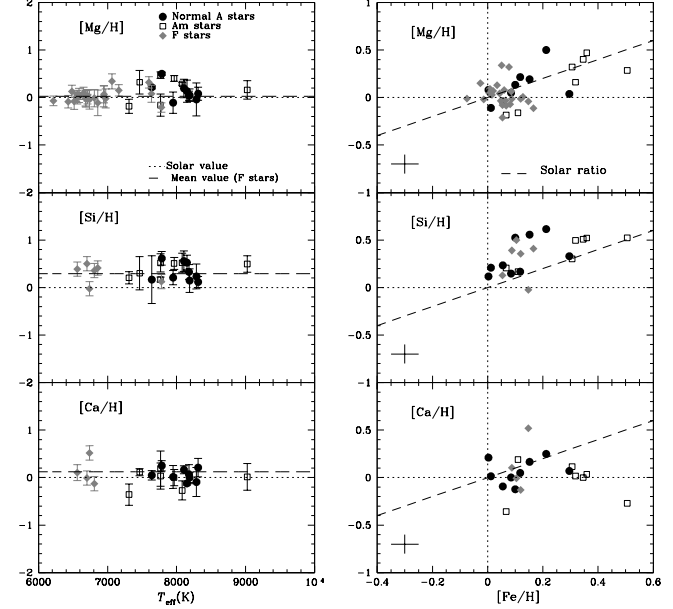


Fig. 9. Left panel: Abundances of magnesium, silicon and calcium versus effective temperature. The dotted line represents the solar value and the dashed one represents the mean abundance of F stars. Right panel: [Mg/H], [Si/H] and [Ca/H] versus [Fe/H]. The symbols are the same as in Figure 8. The dashed lines represent the solar ratios.

for HD 29499 are deficient in scandium and fall in the lower right part of Figure 10. The two stars, HD27962 and HD28355, for which we confirm the status as Am stars, are located in that region.

Titanium, chromium and manganese abundances were derived for A stars only since none of the Ti, Cr and Mn lines observed with AURELIE have oscillator strengths accurate enough for abundance determinations. There does not seem to be significant star-to-star variation in [Ti/H], [Cr/H] nor [Mn/H] for the A stars (Fig.10). The titanium abundances of the Hyades A stars do not appear to be correlated with the iron abundances. The chromium abundance appears to be only loosely correlated to that of iron.

Iron abundances have been derived for all F and A stars of our sample. Neutral iron lines were used for F stars yielding a mean abundance of $\langle [Fe/H] \rangle_F = 0.05 \pm 0.05$ dex. This value, which represents the average metallicity of the cluster, is almost 0.1 dex smaller than the value derived by Boesgaard & Friel (1990) from a different sample of 14 F Dwarfs ($+0.127 \pm 0.022$ dex using different FeI lines from ours). For the 16 A stars, 27 lines of FeII were synthesized. The normal A and Am stars scatter around their mean abundance with a maximum spread of about 0.50 dex, which is more than twice larger than the typical uncertainty on [Fe/H] is about 0.20 dex. This suggests real star-to-star variations in [Fe/H] among the Hyades A stars. Nickel behaves similarly to iron (see Fig. 11), the A stars display large star-to-star variations in [Ni/H] and the abundances are clearly correlated with the iron abundances, the correlation coefficient being close to 1.

All Am stars appear to be overabundant in strontium. Star-

⁶ <http://www.nist.gov/>

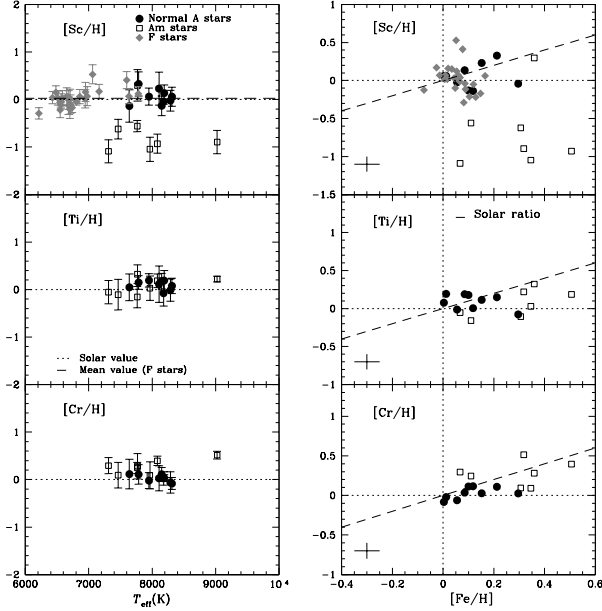


Fig. 10. Left panel: Abundances of scandium, titanium and chromium versus effective temperature. The dotted line represents the solar value and the dashed one represents the mean abundance of F stars. Right panel: $[\text{Sc}/\text{H}]$, $[\text{Ti}/\text{H}]$ and $[\text{Cr}/\text{H}]$ versus $[\text{Fe}/\text{H}]$. The symbols are the same as in Figure 8. The dashed lines represent the solar ratios.

to-star variation in $[\text{Sr}/\text{H}]$ are clearly present. Strontium abundances are only loosely correlated with that of iron (right part of Fig. 12). Yttrium and zirconium are found overabundant in all A stars with a real star-to-star variations in $[\text{Y}/\text{H}]$ and $[\text{Zr}/\text{H}]$ (Figure 12). As for strontium, yttrium and zirconium abundances are correlated to $[\text{Fe}/\text{H}]$ but appear to increase more rapidly than $[\text{Fe}/\text{H}]$ (slope of 1.8 for Y and 2.1 for Zr).

5. Discussion

5.1. Self-consistent evolutionary models

The derived abundances have been compared to the predictions of recent evolutionary models. These models are calculated with the Montréal stellar evolution code. The chemical transport problem is treated with all known physical processes from first principles, which includes radiative accelerations, thermal diffusion and gravitational settling (for more details see Turcotte et al. 1998b, Richard et al. 2001 and references therein). These models follow the chemical evolution of most elements as well as some isotopes up to $Z \leq 28$ (28 species in all). As the abundances change, the Rosseland opacity and radiative accelerations are continuously recalculated at each mesh point and for every time step during evolution which means that the treatment of particle transport is completely self-consistent. The spectra used to calculate the monochromatic opacities are taken from the OPAL database (Iglesias et al. 1996). The radiative accelerations are calculated as described in Richer et al. (1998) with corrections for the redistribution of momentum from Gonzalez et al. (1995)

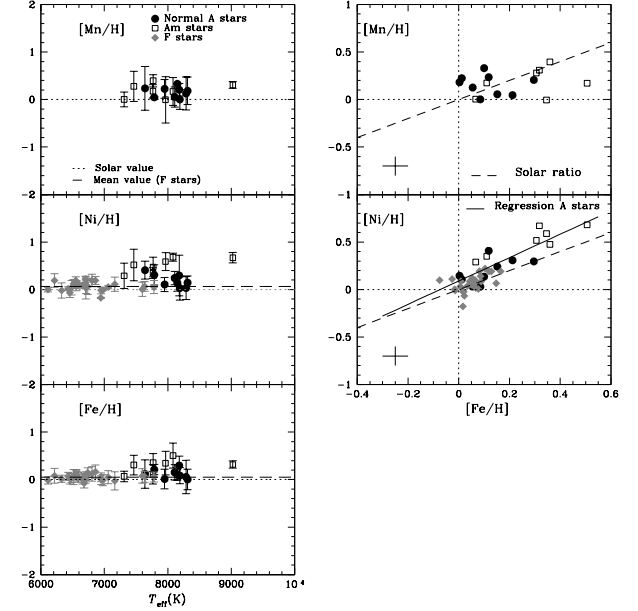


Fig. 11. Left panel: Abundances of manganese, iron and nickel versus effective temperature. The dotted line represents the solar value and the dashed one represents the mean abundance of F stars. Right panel: $[\text{Mn}/\text{H}]$ and $[\text{Ni}/\text{H}]$ versus $[\text{Fe}/\text{H}]$. The symbols are the same as in Figure 8. The dashed lines represent the solar ratios.

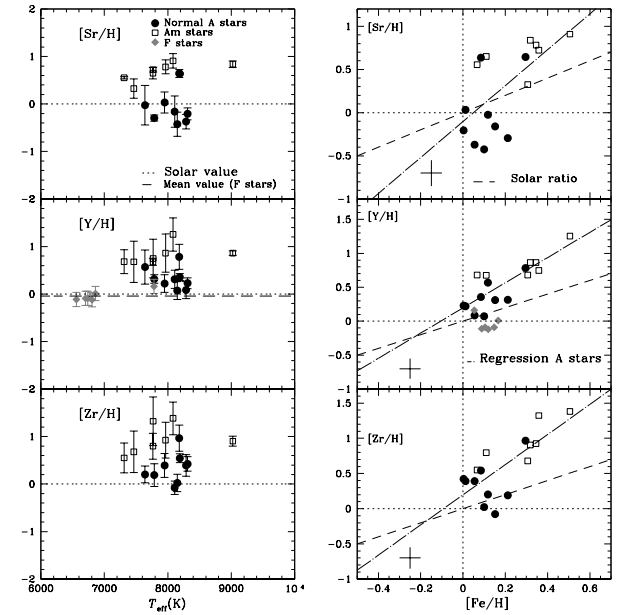


Fig. 12. Left panel: Abundances of strontium, yttrium and zirconium versus effective temperature. Right panel: $[\text{Sr}/\text{H}]$, $[\text{Y}/\text{H}]$ and $[\text{Zr}/\text{H}]$ versus $[\text{Fe}/\text{H}]$. The symbols are the same as in Figure 8.

and LeBlanc et al. (2000). The mixing length parameter and initial helium abundance ($\alpha = 2.096$ and $Y_0 = 0.2779$ respectively) are calibrated to fit the current luminosity and radius of the Sun (see Turcotte et al. 1998b, model H). Models are evolved from the pre-main sequence with a solar scaled abundance mix. The initial abundance ratios are given in Table 1 of Turcotte et al. (1998b). For the initial mass fraction of metals we used both $Z_0 = 0.02$, the solar metal content, and $Z_0 = 0.024$ (to represent the increased metallicity of the Hyades, Lebreton et al. 2001).

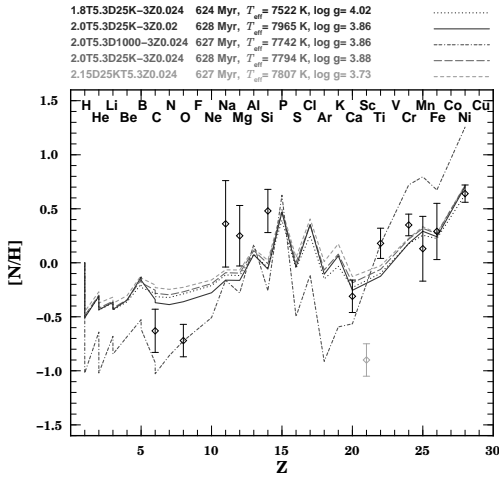


Fig. 13. Comparison of the predicted surface abundances for stars of 1.8 , 2.0 and 2.15 M_\odot with different turbulence prescriptions and different initial metallicities with those derived (depicted as diamonds with their respective uncertainties) for the Am star HD30210 ($T_{\text{eff}} = 8082 \text{ K}$ and $\log g = 3.92$). The gray symbol for Sc indicates that it is not considered in the evolution models.

5.1.1. The A stars

The derived abundances in A stars are compared to the predictions of self-consistent evolutionary models calculated as in Richer et al. (2000). These models include an arbitrary parameter, the amount of mass mixed by turbulent mixing, in order to lower the effects of chemical separation and better fit the abundances of AmFm stars. The effect of turbulence is to extend the mixed mass below the surface convection zone, down to layers where atomic diffusion is less efficient (ie. where time scales are longer due to higher local density). *A priori*, the cause of turbulence is not considered, however it was found to be compatible with rotationally induced turbulence as calculated by Zahn 2005 and Talon et al. 2006. The surface abundances are shown to depend solely on the amount of mass mixed as well as initial metallicity. In Figure 13, we compare the predicted surface abundances for five models with masses of 1.8 , 2.0 and 2.15 M_\odot to the observed abundances of the Hyades A2m star HD30210 ($T_{\text{eff}} = 8082 \text{ K}$ and $\log g = 3.92 \text{ dex}$). The models are shown for both $Z=0.02$ and $Z=0.024$. To help interpret the chosen nomenclature, the $2.0\text{T}5.3\text{D}1000\text{-}3$ corresponds to a 2.0 M_\odot star for which the abundances are completely homogenized down to $\log T = 5.3$. Below this point, as we move deeper inside the star, the turbulent diffusion coefficient $D_T = 1000 D_{\text{He}}$ (the helium diffusion coefficient) decreases as ρ^{-3} ($2.0\text{T}5.3\text{D}25\text{K}-3$ would have the same behavior except that the turbulent coef-

ficient $D_T = 25000 D_{\text{He}}$ at $\log T = 5.3$). It is clear from the plot that the amount of prescribed turbulence has an influence on the surface behavior. The model $2.0\text{T}5.3\text{D}1000\text{-}3$ does not sufficiently impede microscopic diffusion to reproduce most abundances. However, for all other models with greater turbulence, the predicted carbon and oxygen underabundances are not as important as the observed anomalies. The predicted slight underabundances of Na, Mg and Si are not observed in HD30210, but are observed in a few of the Am stars. However the silicon abundance is probably too large. The model that best fits the data is $2.15\text{T}5.3\text{D}25\text{K}-3\text{Z}0.024$, which has a turbulence prescription which was equivalently able to reproduce the observations in Coma Berenices (see Figures 14 and 15 of Paper I). As in Paper I, models with less turbulence roughly replicate the observations for $Z < 12$ and the more turbulent models are better able to reproduce the heavier elements ($Z > 15$). The different metallicities do not lead to significant differences in the predicted abundance patterns, but do have an important effect on T_{eff} .

5.1.2. The F-type stars

For the F dwarfs, we have compared the found abundances to the predicted surface abundances for C, O, Na, Mg, Fe and Ni using Turcotte's evolutionary models at 620 Myr (Turcotte et al. 1998a). These models, calculated for masses ranging from $1.1\text{-}1.5 \text{ M}_\odot$, treat radiative diffusion in detail but do not include macroscopic mixing processes (meridional circulation, turbulence or mass loss). They show that the effects of atomic diffusion, namely the appearance of surface abundance anomalies, can be expected in all stars earlier than F5 ($M_* > 1.3 \text{ M}_\odot$). The found mean carbon abundance for F stars, $\langle [\text{C}/\text{H}] \rangle = -0.09 \text{ dex}$ with very small dispersion, does not agree with predicted underabundance at 620 Myr ($\log \text{age} = 8.79$ in Figure 7 of Turcotte et al. 1998a) and for a 1.4 M_\odot star, representative of the F stars analysed here. The oxygen abundances, which show large scatter for the F stars, can typically be underabundant by -0.41 dex or overabundant by up to 0.28 dex for a 1.4 M_\odot F star (roughly an effective temperature of 6700 K at the age of the Hyades). Again, they do not agree with the predicted surface underabundances [O/H] predicted by Turcotte et al. (1998a). The predicted solar Na abundances match reasonably well of our determinations for F stars. Magnesium is predicted to be slightly underabundant (Fig. 7 of Turcotte et al. 1998a), whereas for most F stars we find overabundances. Finally, iron and nickel are found to be mildly overabundant in case of F stars with $T_{\text{eff}} \in [6600 \text{ K}, 6800 \text{ K}]$ ($\langle [\text{Fe}/\text{H}] \rangle = 0.06 \text{ dex}$ and $\langle [\text{Ni}/\text{H}] \rangle = 0.11 \text{ dex}$). These results disagree with the overabundances of 0.5 and 0.8 dex respectively for a 1.4 M_\odot . As expected, these purely diffusive models typically predict too little C and O and too much iron-peak elements.

6. Conclusion

Selected high quality lines in new high resolution échelle spectra of 16 A and 28 F stars of the Hyades have been synthesized in a uniform manner to derive LTE abundances, a few of which have been corrected for Non-LTE effects whenever possible. Even when binary stars are removed, the abundances of several chemical elements for A stars and early F stars exhibit real star-to-star variations, significantly larger than for the late F stars. The largest spreads occur for Sc, Sr, Y, Zr while the lowest are for Mg, Si and Cr for A stars. Gebran et al (2008) and Gebran & Monier (2008) had already found similar behaviour in the Coma

Berenices and the Pleiades. The derived abundances do not depend on effective temperatures nor apparent rotational velocities as expected since the timescales of diffusion are much shorter than those of rotational mixing (Charbonneau & Michaud 1991). The abundances of Cr, Ni, Sr, Y and Zr are correlated with the iron abundance as was found for the Pleiades and Coma Berenices. The ratios [C/Fe] and [O/Fe] are anticorrelated with [Fe/H] (particularly true for normal A stars). Compared to normal A stars, all Am stars in the Hyades appear to be more deficient in C and O and more overabundant in elements heavier than Fe but not all are deficient in calcium and/or scandium. The F stars have nearly solar abundances for almost all elements except for Si and Ca. The Blue Straggler HD 27962 appears to have abundances characteristic of an Am star (scandium deficiency and enrichment in iron-peak and heavy elements). Conversely our abundance analysis of HD 29499 (A5m) yields normal abundances in Ca and Sc and only moderate enrichment in iron-peak and heavy elements suggesting that this star might be a normal A star. The detailed modelling of the A2m star HD 30210 including radiative diffusion and different amounts of turbulent diffusion reproduces the overall shape of the abundance pattern for this star but not individual abundances. Models with the least turbulence reproduce the abundances of the lightest ($Z < 12$) and those with most turbulence reproduce abundances of elements with $Z > 15$. For a few elements, the discrepancies between derived and predicted abundances could be due to Non-LTE effects. However, the inclusion of competing processes such as different prescriptions of rotational mixing (Zahn 2005) and/or different amounts of mass loss (Vick et al. , in preparation) could well improve the agreement between observed and predicted abundance patterns.

Acknowledgements. We warmly thank the OHP night staff for the support during the observing runs. This research has used the SIMBAD, WEBDA, VALD, NIST and Kurucz databases. MV thanks the Département de physique at l'Université de Montréal as well as the GRAAL at l'Université Montpellier II for financial support and the Réseau Québécois de Calcul de Haute Performance (RQCHP) for providing us with the computational resources required for this work. A special thanks to Georges Michaud and Olivier Richard for their careful reading of the manuscript and useful suggestions. LF received support from the Austrian Science Foundation (FWF project P17890-N2).

References

- Abt, H. A., & Morrell, N. I. 1995, *ApJS*, 99, 135
 Adelman S.J., Pyper D.M., Shore S.N., White R.E. & Warren W.H. 1989, *A&AS*, 81, 221
 Alecian, G. 1996, *A&A*, 310, 872
 Balona, L. A. 1994, *MNRAS*, 268, 119
 Barrado y Navascués, D., & Stauffer, J. R. 1996, *A&A*, 310, 879
 Burkhardt, C., & Coupry, M. F. 2000, *A&A*, 354, 216
 Boesgaard, A. M. 1989, *ApJ*, 336, 798
 Boesgaard, A. M., & Tripicco, M. J. 1986, *ApJ*, 303, 724
 Boesgaard, A. M., & Budge, K. G. 1988, *ApJ*, 332, 410
 Boesgaard, A. M., & Friel, E. D. 1990, *ApJ*, 351, 467
 Castellani, V., Degl'Innocenti, S., Prada Moroni, P. G. & Tordiglione, V. 2002, *MNRAS*, 334, 193
 Cayrel, R., Cayrel, G., Campbell, B., & Dappen, W. 1984, Observational Tests of the Stellar Evolution Theory, 105, 537
 Cayrel de Strobel, G., Crifo, F., & Lebreton, Y. 1997, Hipparcos - Venice '97, 402, 687
 Cayrel de Strobel, G., Soubiran, C., & Ralite, N. 2001, *A&A*, 373, 159
 Castelli, F., & Kurucz, R. L. 2003, IAU Symposium, 210, 20P
 Chaffee, F. H., Jr., Carbon, D. F., & Strom, S. E. 1971, *ApJ*, 166, 593
 Charbonneau, P., & Michaud, G. 1991, *ApJ*, 370, 693
 Conti, P. S. 1965, *ApJ*, 142, 1594
 Dommanget, J., & Nys, O. 1995, Bulletin d'Information du Centre de Donnees Stellaires, 46, 3
 Ersperer, D., & North, P. 2002, *A&A*, 383, 227
 Friel, E. D., & Boesgaard, A. M. 1990, *ApJ*, 351, 480
 Garcia Lopez, R. J., Rebolo, R., Herrero, A., & Beckman, J. E. 1993, *ApJ*, 412, 173
 Gebran, M., PhD Thesis, 2007, UMII
 Gebran, M., Monier, R., & Richard, O. 2008, *A&A*, 479, 189
 Gebran, M., & Monier, R. 2008, *A&A*, 483, 567
 Gigas, D. 1988, *A&A*, 192, 264
 Gonzalez, J.-F., LeBlanc, F., Artru, M.-C., & Michaud, G. 1995, *A&A*, 297, 223
 Grenon, M. 2000, HIPPARCOS and the Luminosity Calibration of the Nearer Stars, 24th meeting of the IAU, Joint Discussion 13, August 2000, Manchester, England, meeting abstract, 13,
 Grevesse, N., & Sauval, A. J. 1998, *Space Science Reviews*, 85, 161
 Griffin, R. F., Griffin, R. E. M., Gunn, J. E., & Zimmerman, B. A. 1985, *AJ*, 90, 609
 Hauck, B. 1977, *Revista Mexicana de Astronomia y Astrofisica*, 2, 231
 Hauck, B., & Mermilliod, M. 1998, *A&AS*, 129, 431
 Hill, G. M. 1995, *A&A*, 294, 536
 Hill, G. M., & Landstreet, J. D. 1993, *A&A*, 276, 142
 Holmberg, J., Nordström, B., & Andersen, J. 2007, *A&A*, 475, 519
 Holweger, H., Steffen, M., & Gigas, D. 1986, *A&A*, 163, 333
 Hubeny, I., & Lanz, T. 1992, *A&A*, 262, 501
 Hui-Bon-Hoa, A., & Alecian, G. 1998, *A&A*, 332, 224
 Iglesias, C. A., & Rogers, F. J. 1996, *ApJ*, 464, 943
 Kurucz, R. L. 1992, *Revista Mexicana de Astronomia y Astrofisica*, vol. 23, 23, 45
 Lambert, D. L., McKinley, L. K., & Roby, S. W. 1986, *PASP*, 98, 927
 Landstreet, J. D., Bagnulo, S., Andretta, V., Fossati, L., Mason, E., Silaj, J., & Wade, G. A. 2007, *A&A*, 470, 685
 LeBlanc, F., Michaud, G., & Richer, J. 2000, *ApJ*, 538, 876
 Lebreton, Y., Fernandes, J., & Lejeune, T. 2001, *A&A*, 374, 540 Badly placed 0's.
 Lemke, M. 1989, *A&A*, 225, 125
 Lemke, M. 1990, *A&A*, 240, 331
 Marigo, P., Girardi, L., Bressan, A. et al. 2008, *A&A*, 482, 883
 Monier, R. 2005, *A&A*, 442, 563
 Moon, T. T., & Dworetsky, M. M. 1985, *MNRAS*, 217, 305
 Napiwotzki, R., Schoenberner, D., & Wenske, V. 1993, *A&A*, 268, 653
 Nissen, P. E. 1981, *A&A*, 97, 145
 Percival, S. M., Salaris, M. & Kilkenney, D. 2003, *A&A*, 400, 541
 Perryman, M. A. C., Brown, A. G. A., Lebreton, Y., et al. 1998, *A&A*, 331, 81
 Renson, P. 1992, *Bulletin d'Information du Centre de Donnees Stellaires*, 40, 97
 Rentzschi-Holm, I. 1996, *A&A*, 312, 966
 Rentzschi-Holm, I. 1997, *A&A*, 317, 178
 Richard, O., Michaud, G., & Richer, J. 2001, *ApJ*, 558, 377
 Richer, J., Michaud, G., Rogers, F., Iglesias, C., Turcotte, S., & LeBlanc, F. 1998, *ApJ*, 492, 833
 Richer, J., Michaud, G., & Turcotte, S. 2000, *ApJ*, 529, 338
 Salaris, M., Weiss, A., & Percival, S. M. 2004, *A&A*, 414, 163
 Shulyak, D., Tsymbal, V., Ryabchikova, T., Stütz, Ch., & Weiss, W. W. 2004, *A&A*, 428, 993
 Smalley, B. 2004, IAU Symposium, 224, 131
 Solano, E., & Fernley, J. 1997, *A&AS*, 122, 131
 Steffen, M. 1985, *A&AS*, 59, 403
 Takeda, Y. 1995, *PASJ*, 47, 287
 Takeda, Y., Han, I., Kang, D.-I., Lee, B.-C., & Kim, K.-M. 2008, Journal of Korean Astronomical Society, 41, 83
 Takeda, Y., Kang, D.-I., Han, I., Lee, B.-C., & Kim, K.-M. 2009, arXiv:0907.1329
 Takeda, Y., & Sadakane, K. 1997, *PASJ*, 49, 367
 Talon, S., Richard, O., & Michaud, G. 2006, *ApJ*, 645, 634
 Taylor, B. J. 2006, *AJ*, 132, 2453
 Thorburn, J. A., Hobbs, L. M., Deliyannis, C. P., & Pinsonneault, M. H. 1993, *ApJ*, 415, 150
 Turcotte, S., Richer, J., & Michaud, G. 1998, *ApJ*, 504, 559
 Turcotte, S., Richer, J., Michaud, G., Iglesias, C. A., & Rogers, F. J. 1998, *ApJ*, 504, 539
 van Leeuwen, F. 2007, *Astrophysics and Space Science Library*, 350,
 Varenne, O. 1999, *A&A*, 341, 233
 Varenne, O., & Monier, R. 1999, *A&A*, 351, 247
 Vick, M., & Michaud, G. 2008, Contributions of the Astronomical Observatory Skalnate Pleso, 38, 135
 Zahn, J.-P. 2005, *EAS Publications Series*, 17, 157

Online Material

Table 5. Abundances relative to hydrogen and to the solar value, for A stars.

HD	SpT	CI	σ_C	OI	σ_O	NaI	σ_{Na}	MgII	σ_{Mg}	SiIII	σ_{Si}
HD27628	A3m	-0.69	0.14	-0.16	0.04	0.03	0.25	-0.18	0.15	0.21	0.13
HD27819	A7V	0.01	0.04	-0.26	0.11	-0.03	0.13	0.05	0.13	0.15	0.25
HD27934	A7V	0.01	0.08	0.18	0.13	-0.08	0.25	-0.04	0.34	0.23	0.26
HD27962	A2IV	-0.39	0.13	-0.34	0.05	0.31	0.18	0.16	0.19	0.50	0.17
HD28226	A3m	-0.09	0.19	-0.07	0.06	0.20	0.13	0.32	0.25	0.30	0.35
HD28319	A7III	-0.04	0.10	0.11	0.18	0.13	0.27	-0.11	0.22	0.21	0.15
HD28355	A7V	-0.29	0.07	0.35	0.40	0.54	0.22	0.40	0.06	0.51	0.13
HD28527	A6IV	-0.17	0.09	-0.23	0.20	-0.01	0.28	0.04	0.10	0.33	0.15
HD28546	A5m	-0.22	0.16	-0.44	0.20	0.20	0.05	-0.16	0.23	0.17	0.05
HD28910	A8V	-0.03	0.23	0.14	0.30	0.46	0.27	0.21	0.03	0.17	0.50
HD29388	A6V	-0.01	0.07	0.23	0.18	-0.10	0.20	0.08	0.14	0.12	0.12
HD29499	A5m	0.01	0.14	0.05	0.20	0.52	0.20	0.47	0.07	0.52	0.19
HD29488	A5V	-0.04	0.14	0.26	0.20	0.39	0.43	0.13	0.23	0.52	0.15
HD30210	Am	-0.55	0.19	-0.58	0.20	0.40	0.22	0.29	0.03	0.52	0.20
HD30780	A7V	-0.01	0.18	0.12	0.01	0.18	0.28	0.50	0.03	0.61	0.14
HD32301	A7V	0.03	0.10	0.21	0.19	0.16	0.24	0.19	0.19	0.56	0.21
Procyon	F5IV-V	-0.05	0.09	-0.09	0.10	-0.03	0.18	0.02	0.07	0.10	0.05
HD	SpT	CaII	σ_{Ca}	ScII	σ_{Sc}	TiII	σ_{Ti}	CrII	σ_{Cr}	MnI	σ_{Mn}
HD27628	A3m	-0.36	0.22	-1.09	0.24	-0.05	0.25	0.29	0.17	0.00	0.16
HD27819	A7V	0.00	0.10	0.13	0.17	0.19	0.21	0.03	0.07	0.00	0.21
HD27934	A7V	-0.09	0.31	-0.02	0.22	-0.01	0.35	-0.06	0.22	0.12	0.35
HD27962	A2IV	0.02	0.28	-0.90	0.25	0.22	0.06	0.51	0.08	0.31	0.07
HD28226	A3m	0.11	0.07	-0.62	0.21	-0.11	0.32	0.09	0.27	0.28	0.31
HD28319	A7III	0.01	0.24	0.06	0.18	0.19	0.14	-0.02	0.17	0.22	0.20
HD28355	A7V	0.00	0.17	-1.05	0.25	0.03	0.26	0.09	0.28	-0.01	0.49
HD28527	A6IV	0.07	0.20	-0.04	0.06	-0.08	0.27	0.02	0.14	0.21	0.13
HD28546	A5m	0.19	0.37	-0.56	0.12	-0.16	0.22	0.25	0.12	0.17	0.14
HD28910	A8V	0.05	0.10	-0.14	0.34	0.05	0.28	0.12	0.31	0.24	0.46
HD29388	A6V	0.21	0.19	0.06	0.20	0.08	0.16	-0.08	0.13	0.18	0.29
HD29499	A5m	0.03	0.27	0.30	0.33	0.32	0.20	0.28	0.27	0.40	0.13
HD29488	A5V	-0.12	0.03	-0.13	0.21	0.15	0.14	0.11	0.14	0.33	0.20
HD30210	Am	-0.27	0.20	-0.93	0.20	0.19	0.14	0.39	0.10	0.17	0.29
HD30780	A7V	0.25	0.11	0.33	0.25	0.11	0.22	0.11	0.20	0.05	0.01
HD32301	A7V	0.16	0.08	0.23	0.35	0.11	0.38	0.03	0.27	0.06	0.21
Procyon	F5IV-V	-0.08	0.10	0.10	0.07	0.11	0.09	-0.08	0.07	0.10	0.04
HD	SpT	FeII	σ_{Fe}	NiI	σ_{Ni}	SrII	σ_{Sr}	YII	σ_Y	ZrII	σ_{Zr}
HD27628	A3m	0.07	0.11	0.29	0.26	0.55	0.02	0.68	0.25	0.55	0.31
HD27819	A7V	0.08	0.17	0.03	0.25	0.64	0.01	0.36	0.07	0.54	0.09
HD27934	A7V	0.05	0.35	0.03	0.24	-0.37	0.15	0.08	0.18	0.39	0.23
HD27962	A2IV	0.32	0.08	0.67	0.11	0.84	0.07	0.86	0.05	0.90	0.10
HD28226	A3m	0.31	0.21	0.52	0.33	0.32	0.20	0.68	0.43	0.68	0.43
HD28319	A7III	0.01	0.21	0.11	0.15	0.03	0.22	0.22	0.19	0.39	0.25
HD28355	A7V	0.35	0.25	0.59	0.19	0.78	0.15	0.86	0.40	0.92	0.38
HD28527	A6IV	0.30	0.20	0.30	0.43	0.64	0.08	0.78	0.26	0.97	0.28
HD28546	A5m	0.11	0.20	0.35	0.11	0.65	0.12	0.68	0.07	0.80	0.27
HD28910	A8V	0.12	0.30	0.41	0.19	-0.02	0.41	0.57	0.36	0.20	0.18
HD29388	A6V	0.00	0.22	0.14	0.14	-0.21	0.12	0.23	0.11	0.42	0.15
HD29499	A5m	0.36	0.19	0.47	0.21	0.72	0.05	0.75	0.41	1.32	0.51
HD29488	A5V	0.10	0.11	0.14	0.17	-0.42	0.25	0.07	0.19	0.02	0.18
HD30210	Am	0.51	0.26	0.68	0.08	0.91	0.15	1.25	0.35	1.38	0.34
HD30780	A7V	0.21	0.10	0.31	0.21	-0.29	0.06	0.31	0.09	0.19	0.24
HD32301	A7V	0.15	0.16	0.24	0.14	-0.16	0.33	0.31	0.19	-0.08	0.14
Procyon	F5IV-V	0.03	0.04	-0.12	0.19	0.25	0.06	0.10	0.12	0.15	0.11

Table 6. Abundances relative to hydrogen and to the solar value, for F stars.

HD	SpT	CI	σ_c	OI	σ_o	NaI	σ_{Na}	MgI	σ_{Mg}	SiII	σ_{Si}	CaII	σ_{Ca}
HD18404	F5IV	-0.20	0.16	-0.41	0.20	-0.08	0.12	-0.04	0.20	-0.02	0.14	0.52	0.17
HD24357	F4V			-0.28	0.16	0.31	0.15	-0.02	0.20				
HD25102	F5V			0.200	0.20	0.35	0.32	-0.01	0.17				
HD26015	F3V	0.23	0.15	-0.01	0.18	0.03	0.07	-0.11	0.22	0.41	0.18		
HD26345	F6V			-0.10	0.20	0.04	0.04	-0.03	0.17				
HD26462	F4V			-0.08	0.17	-0.09	0.28	0.03	0.21				
HD26911	F5V	-0.14	0.14	0.16	0.19	0.04	0.09	-0.01	0.18	0.36	0.13	-0.13	0.19
HD27383	F9V			-0.34	0.19	-0.01	0.03	-0.07	0.10				
HD27459	F0V			-0.04	0.13	0.47	0.06	-0.21	0.10	0.13	0.16		
HD27524	F5V			0.24	0.18	0.15	0.29	-0.08	0.17				
HD27534	F5V			0.28	0.17	0.01	0.02	0.13	0.13				
HD27561	F5V			-0.04	0.15	0.00	0.05	-0.03	0.10				
HD27848	F8			-0.06	0.14	-0.02	0.02	0.06	0.09				
HD27991	F7V			-0.40	0.15	0.09	0.01	-0.09	0.13				
HD28363	F8V			-0.34	0.20	0.14	0.01						
HD28406	F8V	-0.17	0.19	-0.22	0.21	-0.01	0.05	-0.01	0.12	0.39	0.10	0.10	0.18
HD28556	F0V			-0.08	0.06			0.08	0.18				
HD28568	F2			0.18	0.20	0.27	0.24	0.04	0.12				
HD28677	F4V			0.01	0.15			0.34	0.16				
HD28736	F5V			0.28	0.20	-0.06	0.15	0.09	0.13				
HD28911	F2			0.26	0.21	0.21	0.25	0.04	0.15				
HD29169	F5IV			0.18	0.17	0.46	0.05	0.07	0.18				
HD29225	F8	-0.190	0.14	0.19	0.20	0.17	0.24			0.50	0.17	-0.01	0.12
HD30034	F0V			-0.15	0.05	0.50	0.01	0.32	0.12				
HD30810	F6V			-0.06	0.17	0.04	0.01						
HD30869	F5			0.00	0.20	-0.01	0.09						
HD31236	F3IV			-0.04	0.12	-0.06	0.15	0.15	0.12				
HD31845	F5V			-0.24	0.20	-0.06	0.02	0.01	0.10				
HD	SpT	ScII	σ_{Sc}	FeI	σ_{Fe}	NiI	σ_{Ni}	YII	σ_Y				
HD18404	F5IV	-0.17	0.10	0.15	0.10	0.06	0.17	-0.09	0.21				
HD24357	F4V	0.07	0.20	-0.01	0.12	-0.01	0.01						
HD25102	F5V	-0.12	0.19	-0.07	0.10	0.10	0.02						
HD26015	F3V	0.06	0.15	0.17	0.14	0.19	0.08	0.01	0.24				
HD26345	F6V	-0.01	0.20	0.06	0.07	0.10	0.02						
HD26462	F4V	0.01	0.19	0.02	0.06	-0.18	0.00						
HD26911	F5V	-0.05	0.07	0.12	0.15	0.19	0.13	-0.12	0.18				
HD27383	F9V	-0.29	0.12	0.08	0.16	0.19	0.14						
HD27459	F0V	0.12	0.15	0.05	0.10	0.05	0.14	0.16	0.13				
HD27524	F5V	0.03	0.15	0.05	0.16	0.12	0.09						
HD27534	F5V	0.15	0.14	0.03	0.09	0.04	0.15						
HD27561	F5V	-0.10	0.20	0.05	0.06	0.06	0.14						
HD27848	F8	-0.04	0.16	0.09	0.08	0.14	0.04						
HD27991	F7V	0.04	0.13	0.07	0.08	0.02	0.04						
HD28363	F8V			0.02	0.07	-0.02	0.16						
HD28406	F8V	-0.11	0.05	0.09	0.12	0.08	0.10	-0.11	0.11				
HD28556	F0V	0.07	0.16	0.06	0.12	0.07	0.10						
HD28568	F2	0.01	0.20	0.01	0.08	0.03	0.23						
HD28677	F4V	0.53	0.20	0.05	0.14	0.05	0.03						
HD28736	F5V	0.07	0.18	0.01	0.10	0.08	0.03						
HD28911	F2	0.03	0.16	0.04	0.10	0.09	0.05						
HD29169	F5IV	0.16	0.20	0.02	0.12	-0.02	0.07						
HD29225	F8	-0.21	0.19	0.10	0.06	0.22	0.06	-0.09	0.15				
HD30034	F0V	0.41	0.18	0.08	0.15	0.01	0.15						
HD30810	F6V			-0.02	0.08	0.00	0.05						
HD30869	F5			0.02	0.11	-0.06	0.10						
HD31236	F3IV	0.17	0.15	-0.03	0.19	0.11	0.15						
HD31845	F5V	-0.22	0.16	0.13	0.07	0.19	0.08						

Table 7. Absolute parameters for the observed stars.

Star	L/L_\odot	σ_L	$\log T_{\text{eff}}$	$\sigma_{\log T_{\text{eff}}}$	Mass (M_\odot)	σ_M	Fr. age	$\sigma_{\text{Fr.age}}$
HD27628	0.97	0.05	3.864	0.007	1.71	0.12	0.36	0.05
HD27819	1.31	0.05	3.913	0.007	2.05	0.10	0.63	0.09
HD27934	1.54	0.05	3.918	0.007	2.28	0.16	0.83	0.13
HD27962	1.47	0.05	3.955	0.006	2.27	0.23	0.83	0.13
HD28226	0.97	0.05	3.873	0.007	1.73	0.09	0.37	0.06
HD28319	1.89	0.05	3.900	0.007	2.58	0.18	1.05	0.16
HD28355	1.23	0.05	3.901	0.007	1.96	0.10	0.55	0.08
HD28527	1.32	0.05	3.913	0.007	2.06	0.10	0.64	0.10
HD28546	1.06	0.05	3.890	0.007	1.81	0.09	0.43	0.06
HD28910	1.39	0.05	3.883	0.007	2.09	0.21	0.66	0.11
HD29388	1.52	0.05	3.920	0.007	2.27	0.16	0.83	0.12
HD29499	1.09	0.05	3.890	0.007	1.83	0.09	0.44	0.07
HD29488	1.35	0.05	3.911	0.007	2.08	0.09	0.66	0.10
HD30210	1.09	0.05	3.908	0.007	1.86	0.19	0.46	0.07
HD30780	1.20	0.05	3.891	0.007	1.92	0.10	0.51	0.08
HD32301	1.38	0.05	3.909	0.007	2.11	0.11	0.68	0.10
HD24357	0.87	0.05	3.843	0.008	1.61	0.11	0.30	0.04
HD25102	0.70	0.05	3.825	0.008	1.47	0.10	0.23	0.03
HD26015	0.85	0.05	3.836	0.008	1.58	0.11	0.28	0.04
HD26345	0.60	0.05	3.825	0.008	1.44	0.07	0.22	0.03
HD26462	0.97	0.05	3.842	0.008	1.68	0.17	0.34	0.05
HD26911	0.73	0.05	3.833	0.008	1.51	0.11	0.25	0.04
HD27383	0.48	0.05	3.793	0.009	1.29	0.13	0.17	0.03
HD27459	1.14	0.05	3.891	0.007	1.88	0.13	0.48	0.07
HD27524	0.53	0.05	3.814	0.008	1.37	0.07	0.19	0.03
HD27534	0.53	0.05	3.812	0.008	1.37	0.07	0.19	0.03
HD27561	0.61	0.05	3.827	0.008	1.45	0.07	0.22	0.03
HD27848	0.46	0.05	3.817	0.008	1.37	0.07	0.19	0.03
HD27991	0.66	0.05	3.808	0.008	1.42	0.10	0.21	0.03
HD28363	0.60	0.05	3.810	0.009	1.38	0.10	0.20	0.03
HD28406	0.48	0.05	3.817	0.008	1.37	0.07	0.19	0.03
HD28556	1.09	0.05	3.883	0.007	1.82	0.13	0.43	0.06
HD28568	0.65	0.05	3.827	0.008	1.46	0.07	0.23	0.03
HD28677	0.85	0.05	3.849	0.008	1.61	0.08	0.30	0.04
HD28736	0.69	0.05	3.823	0.008	1.46	0.10	0.23	0.03
HD28911	0.60	0.05	3.819	0.008	1.42	0.07	0.21	0.03
HD29169	0.85	0.05	3.842	0.008	1.59	0.11	0.29	0.04
HD29225	0.59	0.05	3.826	0.008	1.43	0.07	0.21	0.03
HD30034	1.09	0.05	3.881	0.007	1.82	0.13	0.43	0.06
HD30810	0.52	0.05	3.786	0.009	1.31	0.13	0.17	0.03
HD30869	0.74	0.05	3.810	0.008	1.47	0.15	0.23	0.04
HD31236	0.71	0.05	3.855	0.008	1.56	0.16	0.27	0.04
HD31845	0.55	0.05	3.816	0.008	1.38	0.06	0.20	0.03
HD18404	0.93	0.05	3.829	0.008	1.63	0.16	0.31	0.05

Table 8. Elemental abundances for each line of each chemical element for A and F stars.

A stars HD27628							
λC	log(C/H) $_{\star}$	λO	log(O/H) $_{\star}$	λNa	log(Na/H) $_{\star}$	λMg	log(Mg/H) $_{\star}$
4932.049	7.774	5330.700	8.700	4668.559	5.900	4390.510	7.207
5052.167	7.759	6158.1	8.560	4982.813	6.547	4481.1	7.503
5380.337	7.605			6154.226	6.386		
5793.120	8.005			6160.747	6.456		
λSi	log(Si/H) $_{\star}$	λCa	log(Ca/H) $_{\star}$	λSc	log(Sc/H) $_{\star}$	λTi	log(Ti/H) $_{\star}$
5055.984	7.844	5001.479	5.722	4314.083	2.086	4163.644	5.407
5978.930	7.521	5019.971	5.900	4324.996	1.762	4287.873	5.009
6347.110	7.818	5285.266	6.264	5031.021	2.089	4300.042	4.708
6371.371	7.681			5239.813	2.416	4386.844	5.004
				5526.790	1.848	4394.059	4.690
						4395.051	4.730
						4399.772	5.104
						4443.801	4.576
						4468.492	4.849
						4501.270	4.928
						4805.085	5.187
λCr	log(Cr/H) $_{\star}$	λMn	log(Mn/H) $_{\star}$	λFe	log(Fe/H) $_{\star}$	λNi	log(Ni/H) $_{\star}$
4592.049	6.283	4033.062	5.200	4273.326	7.506	4470.472	6.427
4616.629	5.758	4034.483	5.168	4416.830	7.406	4604.982	6.375
4634.070	5.747	4055.544	5.303	4491.405	7.583	5080.528	6.363
4812.337	5.899	4083.628	5.625	4508.288	7.496	5099.927	6.201
5237.329	5.866	4754.042	5.369	4515.339	7.530	5476.904	7.031
5308.440	5.913	4783.427	5.455	4520.224	7.745	6176.807	6.603
5313.590	6.000			4522.634	7.488		
				4541.524	7.657		
				4555.890	7.463		
				4582.835	7.643		
				4620.521	7.499		
				4923.927	7.702		
				5197.577	7.472		
				5276.002	7.143		
				5316.615	7.567		
λSr	log(Sr/H) $_{\star}$	λY	log(Y/H) $_{\star}$	λZr	log(Zr/H) $_{\star}$		
4077.709	3.461	4883.684	2.727	4149.217	2.671		
4215.520	3.507	4900.120	3.317	4156.240	3.449		
		5087.416	2.696	4161.210	3.485		
		5200.406	2.790	4208.980	3.042		
				4496.980	2.906		

HD27819

λC	log(C/H) $_{\star}$	λO	log(O/H) $_{\star}$	λNa	log(Na/H) $_{\star}$	λMg	log(Mg/H) $_{\star}$
4932.049	8.430	5330.700	8.402	4668.559	6.273	4390.510	7.471
5052.167	8.505	6155.900	8.644	4982.813	6.084	4427.994	7.525
5380.337	8.496	6156.750	8.423	6154.226	6.412	4481.1	7.772
5793.120	8.541	6158.100	8.633				
λSi	log(Si/H) $_{\star}$	λCa	log(Ca/H) $_{\star}$	λSc	log(Sc/H) $_{\star}$	λTi	log(Ti/H) $_{\star}$
5055.984	7.652	5001.479	6.450	4314.083	3.059	4163.644	5.284
5978.930	7.281	5019.971	6.346	4320.732	3.483	4287.873	4.959
6347.110	7.981	5021.138	6.158	4324.996	3.428	4300.042	5.239
6371.371	7.716	5285.266	6.330	5031.021	3.158	4386.844	4.893
				5239.813	3.314	4394.059	4.779
				5526.790	3.149	4395.051	5.300
						4399.772	5.279
						4417.714	5.092
						4468.492	5.096

Table 8. continued.

λ Cr	log(Cr/H) $_{\star}$	λ Mn	log(Mn/H) $_{\star}$	λ Fe	log(Fe/H) $_{\star}$	λ Ni	log(Ni/H) $_{\star}$
4592.049	5.649	4033.062	5.137	4273.326	7.307	4470.472	5.750
4634.070	5.647	4034.483	5.163	4296.570	7.580	4604.982	6.340
4812.337	5.729	4083.628	5.726	4416.830	7.114	5080.528	6.269
5237.329	5.663	4754.042	5.357	4491.405	7.498	5099.927	6.535
5308.440	5.539	4783.427	5.377	4508.288	7.564	5476.904	6.404
5313.590	5.764			4515.339	7.567	6176.807	6.139
				4520.224	7.623		
				4522.634	7.557		
				4541.524	7.527		
				4555.890	7.869		
				4666.758	7.654		
				4923.927	7.719		
				5197.577	7.395		
				5276.002	7.656		
				5316.615	7.548		
λ Sr	log(Sr/H) $_{\star}$	λ Y	log(Y/H) $_{\star}$	λ Zr	log(Zr/H) $_{\star}$		
4077.709	3.581	4883.684	2.600	4149.217	3.033		
4215.520	3.552	4900.120	2.652	4156.240	3.040		
		5087.416	2.489	4208.980	3.260		
		5200.406	2.482	4496.980	3.080		

HD27934

λ C	log(C/H) $_{\star}$	λ O	log(O/H) $_{\star}$	λ Na	log(Na/H) $_{\star}$	λ Mg	log(Mg/H) $_{\star}$
4932.049	8.515	5330.700	9.187	4668.559	6.603	4390.510	7.635
5052.167	8.363	6156.750	8.910	4982.813	5.907	4427.994	7.026
5380.337	8.523	6158.1	8.880	6154.226	6.305	4481.1	7.839
5793.120	8.580			6160.747	6.028		
λ Si	log(Si/H) $_{\star}$	λ Ca	log(Ca/H) $_{\star}$	λ Sc	log(Sc/H) $_{\star}$	λ Ti	log(Ti/H) $_{\star}$
5055.984	7.739	4472.050	5.702	4314.083	3.255	4163.644	4.466
5978.930	7.336	5001.479	6.272	4320.732	3.062	4287.873	4.677
6347.110	8.053	5019.971	6.167	4324.996	3.475	4300.042	5.045
6371.371	7.849	5021.138	6.640	5031.021	2.890	4386.844	4.779
		5285.266	6.355	5239.813	2.953	4395.051	5.129
				5526.790	3.006	4399.772	5.347
						4417.714	4.888
						4443.801	5.152
						4468.492	4.896
						4501.270	5.130
						4805.085	5.123
λ Cr	log(Cr/H) $_{\star}$	λ Mn	log(Mn/H) $_{\star}$	λ Fe	log(Fe/H) $_{\star}$	λ Ni	log(Ni/H) $_{\star}$
4592.049	5.413	4033.062	5.021	4273.326	6.923	4470.472	5.823
4616.629	5.365	4034.483	5.120	4416.830	7.745	5080.528	6.132
4634.070	5.774	4083.628	5.946	4491.405	7.077	5099.927	6.357
4812.337	5.917	4783.427	5.362	4508.288	7.477	5476.904	6.425
5237.329	5.495			4515.339	7.377	6176.807	6.472
5308.440	5.337			4520.224	7.860		
5313.590	5.680			4522.634	7.050		
				4541.524	7.978		
				4555.890	8.012		
				4582.835	7.994		
				4666.758	7.687		
				4923.927	7.633		
				5197.577	7.154		
				5276.002	7.336		
				5316.615	7.422		

Table 8. continued.

λ Sr	log(Sr/H) $_{\star}$	λ Y	log(Y/H) $_{\star}$	λ Zr	log(Zr/H) $_{\star}$
4077.709	2.709	4883.684	2.507	4149.217	2.675
4215.520	2.408	4900.120	2.372	4156.240	3.017
		5087.416	2.253	4156.240	3.030
		5200.406	2.009	4208.980	3.300
				4496.980	2.737

HD27962

λ C	log(C/H) $_{\star}$	λ O	log(O/H) $_{\star}$	λ Na	log(Na/H) $_{\star}$	λ Mg	log(Mg/H) $_{\star}$
4932.049	8.140	5330.700	8.369	4982.813	6.343	4390.510	7.611
5052.167	8.079	6155.900	8.446	6154.226	6.731	4427.994	7.520
5380.337	7.890	6156.750	8.484	6160.747	6.716	4481.1	7.972
5793.120	8.237	6158.1	8.494				
λ Si	log(Si/H) $_{\star}$	λ Ca	log(Ca/H) $_{\star}$	λ Sc	log(Sc/H) $_{\star}$	λ Ti	log(Ti/H) $_{\star}$
5055.984	7.893	4472.050	6.896	4314.083	1.924	4163.644	5.144
5978.930	7.809	5001.479	6.189	4320.732	2.324	4287.873	5.201
6347.110	8.261	5019.971	6.258	5239.813	2.585	4300.042	5.257
6371.371	8.060	5021.138	6.184	5526.790	2.102	4386.844	5.169
		5285.266	6.152			4394.059	5.150
						4395.051	5.188
						4399.772	5.264
						4417.714	5.095
						4443.801	5.185
						4468.492	5.197
						4501.270	5.250
						4805.085	5.316
λ Cr	log(Cr/H) $_{\star}$	λ Mn	log(Mn/H) $_{\star}$	λ Fe	log(Fe/H) $_{\star}$	λ Ni	log(Ni/H) $_{\star}$
4592.049	6.157	4033.062	5.612	4273.326	7.706	4470.472	6.830
4616.629	6.144	4034.483	5.535	4416.830	7.827	4470.472	6.819
4634.070	6.296	4055.544	5.685	4491.405	7.712	5080.528	6.808
4812.337	6.136	4083.628	5.652	4508.288	7.718	5099.927	6.766
5237.329	6.091	4754.042	5.724	4515.339	7.700	5476.904	7.050
5308.440	6.025	4783.427	5.741	4520.224	7.768	6176.807	7.015
5313.590	6.166			4522.634	7.794		
				4541.524	7.742		
				4555.890	7.791		
				4582.835	7.987		
				4666.758	7.795		
				4923.927	7.722		
				5197.577	7.856		
λ Sr	log(Sr/H) $_{\star}$	λ Y	log(Y/H) $_{\star}$	λ Zr	log(Zr/H) $_{\star}$		
4077.709	3.698	4883.684	3.045	4149.217	3.405		
4215.520	3.838	4900.120	3.141	4156.240	3.623		
		5087.416	3.056	4156.240	3.427		
		5200.406	3.011	4208.980	3.327		
				4496.980	3.541		

HD28226

λ C	log(C/H) $_{\star}$	λ O	log(O/H) $_{\star}$	λ Na	log(Na/H) $_{\star}$	λ Mg	log(Mg/H) $_{\star}$
4932.049	8.204	6155.900	8.810	4982.813	6.620	4390.510	7.576
5052.167	8.253	6158.1	8.650	6154.226	6.363	4427.994	8.180
5380.337	8.408					4481.1	7.830
5793.120	8.680						

Table 8. continued.

λSi	$\log(Si/H)_*$	λCa	$\log(Ca/H)_*$	λSc	$\log(Sc/H)_*$	λTi	$\log(Ti/H)_*$
5055.984	7.828	5001.479	6.360	4314.083	2.782	4163.644	4.275
5978.930	7.240	5019.971	6.510	4320.732	2.280	4287.873	5.167
6347.110	8.165			4324.996	2.463	4300.042	4.590
6371.371	8.017					4386.844	4.574
						4395.051	4.926
						4399.772	4.650
						4417.714	5.058
						4443.801	5.439
						4468.492	4.730
						4501.270	5.179
						4805.085	5.030
λSr	$\log(Sr/H)_*$	λY	$\log(Y/H)_*$	λZr	$\log(Zr/H)_*$		
4077.709	3.458	4883.684	3.279	4149.217	2.854		
4215.520	3.052	4900.120	3.319	4156.240	3.200		
		5087.416	2.615	4161.210	3.426		
		5200.406	2.303	4496.980	2.900		

HD28319

λC	$\log(C/H)_*$	λO	$\log(O/H)_*$	λNa	$\log(Na/H)_*$	λMg	$\log(Mg/H)_*$
4932.049	8.352	5330.700	9.200	4982.813	6.580	4390.510	7.474
5052.167	8.350	6155.900	8.800	6154.226	6.025	4427.994	7.139
5380.337	8.480	6156.750	8.850	6160.747	6.728	4481.1	7.681
5793.120	8.595	6158.1	8.740	4668.559	6.335		
λSi	$\log(Si/H)_*$	λCa	$\log(Ca/H)_*$	λSc	$\log(Sc/H)_*$	λTi	$\log(Ti/H)_*$
5055.984	7.604	5001.479	6.148	4314.083	3.530	4163.644	5.240
5978.930	7.540	5019.971	6.220	4320.732	3.098	4287.873	4.951
6347.110	7.903	5021.138	6.220	4324.996	3.147	4300.042	4.982
6371.371	7.828	5285.266	6.748	5031.021	2.970	4386.844	5.256
				5239.813	3.103	4394.059	5.256
				5526.790	3.293	4395.051	5.329
						4399.772	5.016
						4417.714	5.270
						4443.801	4.981
						4468.492	5.311
						4501.270	5.287
						4805.085	5.200

Table 8. continued.

λCr	$\log(\text{Cr}/\text{H})_{\star}$	λMn	$\log(\text{Mn}/\text{H})_{\star}$	λFe	$\log(\text{Fe}/\text{H})_{\star}$	λNi	$\log(\text{Ni}/\text{H})_{\star}$
4592.049	5.432	4033.062	5.603	4273.326	7.747	4470.472	6.094
4616.629	5.503	4034.483	5.603	4416.830	7.451	5080.528	6.172
4634.070	5.750	4055.544	5.821	4491.405	7.443	5099.927	6.362
4812.337	5.880	4083.628	5.270	4508.288	7.426	5476.904	6.328
5237.329	5.468			4515.339	7.290	6176.807	6.394
5308.440	5.536			4520.224	7.350		
5313.590	5.694			4522.634	7.726		
				4541.524	7.665		
				4555.890	7.648		
				4582.835	7.042		
				4666.758	7.320		
				4923.927	7.302		
				5197.577	7.726		
λSr	$\log(\text{Sr}/\text{H})_{\star}$	λY	$\log(\text{Y}/\text{H})_{\star}$	λZr	$\log(\text{Zr}/\text{H})_{\star}$		
4077.709	3.184	4883.684	2.660	4149.217	2.607		
4215.520	2.740	4900.120	2.530	4156.240	3.200		
		5087.416	2.310	4156.240	3.180		
		5200.406	2.180	4496.980	2.820		

HD28355

λC	$\log(\text{C}/\text{H})_{\star}$	λO	$\log(\text{O}/\text{H})_{\star}$	λNa	$\log(\text{Na}/\text{H})_{\star}$	λMg	$\log(\text{Mg}/\text{H})_{\star}$
λSi	$\log(\text{Si}/\text{H})_{\star}$	λCa	$\log(\text{Ca}/\text{H})_{\star}$	λSc	$\log(\text{Sc}/\text{H})_{\star}$	λTi	$\log(\text{Ti}/\text{H})_{\star}$
4932.049	8.140	5330.700	9.540	4982.813	7.057	4390.510	7.880
5052.167	8.120	6158.1	8.736	6154.226	6.890	4481.1	8.003
5380.337	8.300			6160.747	6.530		
5055.984	7.840	5001.479	6.240	4314.083	2.320	4300.042	4.928
6347.110	8.200	5019.971	6.160	4324.996	1.980	4386.844	4.499
6371.371	8.018	5285.266	6.560	5031.021	2.506	4395.051	4.943
				5239.813	1.527	4399.772	5.076
						4443.801	5.513
						4468.492	4.765
						4501.270	5.266
						4805.085	5.064
λCr	$\log(\text{Cr}/\text{H})_{\star}$	λMn	$\log(\text{Mn}/\text{H})_{\star}$	λFe	$\log(\text{Fe}/\text{H})_{\star}$	λNi	$\log(\text{Ni}/\text{H})_{\star}$
4592.049	6.082	4034.483	4.990	4273.326	7.330	4470.472	6.440
4616.629	5.220	4083.628	6.145	4416.830	7.749	4604.982	6.953
4634.070	6.069	4754.042	4.920	4491.405	7.899	5080.528	6.801
4812.337	5.820	4783.427	5.321	4508.288	7.883	5099.927	6.900
5237.329	5.708			4515.339	8.059	5476.904	6.901
5308.440	5.542			4520.224	8.059		
5313.590	5.600			4522.634	7.843		
				4541.524	8.015		
				4555.890	8.163		
				4582.835	7.620		
				4620.521	7.350		
				4923.927	7.818		
				5197.577	7.687		
λSr	$\log(\text{Sr}/\text{H})_{\star}$	λY	$\log(\text{Y}/\text{H})_{\star}$	λZr	$\log(\text{Zr}/\text{H})_{\star}$		
4077.709	3.860	4883.684	3.340	4149.217	3.040		
4215.520	3.564	4900.120	3.530	4156.240	3.600		
		5087.416	2.880	4161.210	4.040		
		5200.406	2.500	4208.980	3.260		

Table 8. continued.

HD28527							
λC	$\log(C/H)_\star$	λO	$\log(O/H)_\star$	λNa	$\log(Na/H)_\star$	λMg	$\log(Mg/H)_\star$
4932.049	8.258	6158.1	8.560	4668.559	6.560	4390.510	7.479
5052.167	8.234			4982.813	5.995	4427.994	7.545
5380.337	8.440					4481.1	7.710
λSi	$\log(Si/H)_\star$	λCa	$\log(Ca/H)_\star$	λSc	$\log(Sc/H)_\star$	λTi	$\log(Ti/H)_\star$
5055.984	7.650	5001.479	6.390	4314.083	3.183	4163.644	4.797
5978.930	8.030			4324.996	3.072	4287.873	4.378
6347.110	7.840			5031.021	3.008	4300.042	5.004
						4386.844	5.004
						4394.059	5.249
						4395.051	4.752
						4399.772	5.250
						4443.801	4.788
λCr	$\log(Cr/H)_\star$	λMn	$\log(Mn/H)_\star$	λFe	$\log(Fe/H)_\star$	λNi	$\log(Ni/H)_\star$
4592.049	5.786	4033.062	5.490	4273.326	7.370	4470.472	5.720
4616.629	5.460	4034.483	5.490	4416.830	7.570	4604.982	6.690
4634.070	5.810	4055.544	5.780	4491.405	7.855	5080.528	6.490
4812.337	5.690	4083.628	5.465	4508.288	7.798	5099.927	6.620
5237.329	5.470			4515.339	7.770	5476.904	7.010
5308.440	5.570			4520.224	7.810		
5313.590	5.797			4522.634	8.150		
				4541.524	7.770		
				4555.890	7.790		
				4582.835	7.678		
λSr	$\log(Sr/H)_\star$	λY	$\log(Y/H)_\star$	λZr	$\log(Zr/H)_\star$		
4077.709	3.658	4883.684	3.180	4149.217	3.420		
4215.520	3.490	4900.120	3.280	4156.240	3.440		
		5087.416	2.862	4161.210	3.660		
		5200.406	2.612	4208.980	3.970		
				4496.980	3.140		

HD28546

λC	$\log(C/H)_\star$	λO	$\log(O/H)_\star$	λNa	$\log(Na/H)_\star$	λMg	$\log(Mg/H)_\star$
4932.049	8.160	6158.1	8.350	4982.813	6.507	4390.510	7.100
5052.167	8.160			6154.226	6.410	4427.994	7.560
5380.337	8.170			6160.747	6.540	4481.1	7.480
5793.120	8.530						
λSi	$\log(Si/H)_\star$	λCa	$\log(Ca/H)_\star$	λSc	$\log(Sc/H)_\star$	λTi	$\log(Ti/H)_\star$
5055.984	7.679	5001.479	7.000	4314.083	2.500	4163.644	5.100
6347.110	7.740	5019.971	6.430	4324.996	2.650	4287.873	5.010
6371.371	7.614	5285.266	6.100	5031.021	2.580	4300.042	4.780
				5239.813	2.507	4386.844	4.840
				5526.790	2.774	4394.059	4.830
						4395.051	4.890
						4399.772	4.880
						4443.801	4.430
						4468.492	4.350
						4501.270	4.745
						4805.085	4.900

Table 8. continued.

λCr	$\log(\text{Cr}/\text{H})_{\star}$	λMn	$\log(\text{Mn}/\text{H})_{\star}$	λFe	$\log(\text{Fe}/\text{H})_{\star}$	λNi	$\log(\text{Ni}/\text{H})_{\star}$
4592.049	5.650	4033.062	5.380	4273.326	7.500	4470.472	6.430
4616.629	5.835	4034.483	5.680	4416.830	8.100	4604.982	6.536
4634.070	5.819	4055.544	5.406	4491.405	7.510	5080.528	6.520
4812.337	5.939	4083.628	5.750	4508.288	7.530	5099.927	6.538
5237.329	5.917	4754.042	5.430	4515.339	7.423	5476.904	6.770
5308.440	5.920	4783.427	5.500	4520.224	7.540		
5313.590	6.049			4522.634	7.621		
				4541.524	7.740		
				4555.890	7.800		
				4582.835	7.470		
				4620.521	7.690		
				4923.927	7.665		
				5197.577	7.280		
				5276.002	7.426		
				5316.615	7.587		
λSr	$\log(\text{Sr}/\text{H})_{\star}$	λY	$\log(\text{Y}/\text{H})_{\star}$	λZr	$\log(\text{Zr}/\text{H})_{\star}$		
4077.709	3.700	4883.684	2.811	4149.217	3.016		
4215.520	3.460	4900.120	2.840	4156.240	3.700		
		5087.416	2.980	4161.210	3.660		
				4208.980	3.200		
				4496.980	3.210		

HD28910

λC	$\log(\text{C}/\text{H})_{\star}$	λO	$\log(\text{O}/\text{H})_{\star}$	λNa	$\log(\text{Na}/\text{H})_{\star}$	λMg	$\log(\text{Mg}/\text{H})_{\star}$
4932.049	8.600	5330.700	9.240	4668.559	7.100	4390.510	7.790
5052.167	8.160	6158.1	8.630	4982.813	6.450	4481.1	7.720
5380.337	8.570			6154.226	6.710		
5793.120	8.200						
λSi	$\log(\text{Si}/\text{H})_{\star}$	λCa	$\log(\text{Ca}/\text{H})_{\star}$	λSc	$\log(\text{Sc}/\text{H})_{\star}$	λTi	$\log(\text{Ti}/\text{H})_{\star}$
5055.984	7.770	5001.479	6.507	4314.083	3.600	4163.644	4.580
5978.930	7.020	5019.971	6.300	4324.996	3.130	4287.873	4.929
6347.110	8.240	5285.266	6.300	5031.021	2.640	4300.042	4.630
				5239.813	2.730	4386.844	5.115
				5526.790	2.560	4395.051	5.116
						4399.772	5.600
						4443.801	4.840
						4468.492	5.173
						4501.270	5.178
						4805.085	5.115
λCr	$\log(\text{Cr}/\text{H})_{\star}$	λMn	$\log(\text{Mn}/\text{H})_{\star}$	λFe	$\log(\text{Fe}/\text{H})_{\star}$	λNi	$\log(\text{Ni}/\text{H})_{\star}$
4592.049	5.540	4033.062	5.780	4273.326	7.340	4470.472	6.350
4616.629	5.900	4034.483	5.780	4416.830	7.170	4604.982	6.830
4634.070	6.130	4055.544	6.200	4491.405	7.900	5080.528	6.519
4812.337	5.250	4083.628	4.960	4508.288	7.510	5099.927	6.580
5237.329	5.910	4754.042	5.398	4515.339	7.900	5476.904	6.900
				4520.224	7.670	6176.807	6.530
				4522.634	7.180		
				4541.524	7.780		
				4555.890	8.050		
				4582.835	7.800		
				4620.521	7.923		
				4923.927	7.567		
				5197.577	7.190		
				5276.002	7.080		
				5316.615	7.617		

Table 8. continued.

λSr	$\log(Sr/H)_*$	λY	$\log(Y/H)_*$	λZr	$\log(Zr/H)_*$
4077.709	3.320	4883.684	3.200	4149.217	2.510
4215.520	2.490	4900.120	3.020	4156.240	2.820
		5087.416	2.540	4161.210	3.000
		5200.406	2.310	4208.980	2.720

HD29388

λC	$\log(C/H)_*$	λO	$\log(O/H)_*$	λNa	$\log(Na/H)_*$	λMg	$\log(Mg/H)_*$
4932.049	8.420	5330.700	9.200	4668.559	6.190	4390.510	7.634
5052.167	8.396	6158.100	8.841			4427.994	7.445
5380.337	8.530					4481.1	7.780
5793.120	8.560						
λSi	$\log(Si/H)_*$	λCa	$\log(Ca/H)_*$	λSc	$\log(Sc/H)_*$	λTi	$\log(Ti/H)_*$
5055.984	7.743	5001.479	6.819	4314.083	3.240	4163.644	4.822
5978.930	7.510	5019.971	6.300	4324.996	3.147	4287.873	5.027
		5285.266	6.420	5031.021	3.605	4300.042	4.978
				5239.813	2.990	4386.844	4.840
				5526.790	3.129	4395.051	5.145
						4399.772	5.370
						4443.801	4.917
						4468.492	5.139
						4501.270	4.967
						4805.085	5.196
λCr	$\log(Cr/H)_*$	λMn	$\log(Mn/H)_*$	λFe	$\log(Fe/H)_*$	λNi	$\log(Ni/H)_*$
4592.049	5.428	4034.483	5.545	4273.326	7.247	4470.472	6.520
4616.629	5.395	4055.544	5.881	4416.830	7.454	4604.982	6.097
4634.070	5.730	4083.628	5.170	4491.405	7.508	5080.528	6.356
4812.337	5.460			4508.288	7.436	5099.927	6.392
5237.329	5.612			4515.339	7.410	5476.904	6.409
5308.440	5.660			4520.224	7.398		
				4522.634	7.320		
				4541.524	7.244		
				4555.890	7.400		
				4582.835	7.900		
				4620.521	8.040		
				4923.927	7.594		
				5197.577	7.507		
				5276.002	7.207		
				5316.615	7.359		
λSr	$\log(Sr/H)_*$	λY	$\log(Y/H)_*$	λZr	$\log(Zr/H)_*$		
4077.709	2.849	4883.684	2.575	4149.217	2.780		
4215.520	2.599	4900.120	2.489	4156.240	3.120		
		5087.416	2.380	4161.210	3.140		
		5200.406	2.272	4208.980	2.890		

HD29499

λC	$\log(C/H)_*$	λO	$\log(O/H)_*$	λNa	$\log(Na/H)_*$	λMg	$\log(Mg/H)_*$
4932.049	8.340	6158.1	8.840	4668.559	6.806	4390.510	8.080
5052.167	8.370					4427.994	7.920
5380.337	8.580					4481.1	8.034
5793.120	8.680						

Table 8. continued.

λSi	$\log(Si/H)_*$	λCa	$\log(Ca/H)_*$	λSc	$\log(Sc/H)_*$	λTi	$\log(Ti/H)_*$
5055.984	7.867	5001.479	6.670	4314.083	3.948	4163.644	5.570
5978.930	8.300	5019.971	6.001	4324.996	3.670	4287.873	5.460
		5285.266	6.390	5031.021	3.250	4300.042	5.460
				5239.813	3.215	4386.844	5.240
				5526.790	3.050	4394.059	5.055
						4395.051	5.330
						4399.772	5.005
λCr	$\log(Cr/H)_*$	λMn	$\log(Mn/H)_*$	λFe	$\log(Fe/H)_*$	λNi	$\log(Ni/H)_*$
4592.049	6.400	4033.062	5.728	4273.326	7.910	4470.472	6.318
4616.629	5.880	4034.483	5.644	4416.830	7.505	4604.982	6.920
4634.070	6.010	4055.544	5.960	4491.405	7.770	5080.528	6.630
4812.337	5.930	4083.628	5.650	4508.288	7.930	5099.927	6.818
5237.329	5.550			4515.339	7.916	5476.904	6.740
5308.440	5.700			4520.224	7.890		
				4522.634	8.200		
				4541.524	7.960		
				4555.890	7.839		
				4582.835	7.670		
				4620.521	7.728		
				4923.927	7.509		
λSr	$\log(Sr/H)_*$	λY	$\log(Y/H)_*$	λZr	$\log(Zr/H)_*$		
4077.709	3.706	4883.684	2.900	4149.217	3.800		
4215.520	3.600	4900.120	3.610	4156.240	4.700		
		5087.416	2.770	4161.210	3.740		
		5200.406	2.512	4208.980	3.290		

HD29488

λC	$\log(C/H)_*$	λO	$\log(O/H)_*$	λNa	$\log(Na/H)_*$	λMg	$\log(Mg/H)_*$
4932.049	8.528	5330.700	9.250	4668.559	7.115	4390.510	7.375
5052.167	8.310	6158.1	8.850	6160.747	6.250	4427.994	7.700
5380.337	8.620					4481.1	7.946
5793.120	8.300						
λSi	$\log(Si/H)_*$	λCa	$\log(Ca/H)_*$	λSc	$\log(Sc/H)_*$	λTi	$\log(Ti/H)_*$
5055.984	7.880	5001.479	6.150	4314.083	3.340	4163.644	5.060
5978.930	8.190	5019.971	6.220	4324.996	3.013	4287.873	5.222
		5285.266	6.220	5031.021	2.770	4300.042	4.870
				5239.813	2.800	4386.844	5.170
				5526.790	3.073	4395.051	5.420
						4399.772	5.280
λCr	$\log(Cr/H)_*$	λMn	$\log(Mn/H)_*$	λFe	$\log(Fe/H)_*$	λNi	$\log(Ni/H)_*$
4592.049	5.530	4033.062	5.680	4273.326	7.530	4470.472	6.249
4616.629	5.810			4416.830	7.507	4604.982	6.640
4634.070	5.975			4491.405	7.600	5080.528	6.130
4812.337	5.603			4508.288	7.580	5099.927	6.370
5237.329	5.770			4515.339	7.570	5476.904	6.340
5308.440	5.770			4520.224	7.585		
				4522.634	7.420		
				4541.524	7.420		
				4555.890	7.456		
				4582.835	7.770		
				4620.521	7.720		
λSr	$\log(Sr/H)_*$	λY	$\log(Y/H)_*$	λZr	$\log(Zr/H)_*$		
4077.709	2.760	4883.684	2.530	4149.217	2.350		
4215.520	2.250	4900.120	2.200	4156.240	2.790		
		5087.416	2.018	4161.210	2.610		
		5200.406	2.340				

Table 8. continued.

HD30210							
λC	$\log(C/H)_*$	λO	$\log(O/H)_*$	λNa	$\log(Na/H)_*$	λMg	$\log(Mg/H)_*$
4932.049	7.730	5330.700	8.210	4668.559	6.470	4390.510	7.860
5052.167	8.120	6155.900	8.207	4982.813	6.910	4481.1	7.792
		6156.750	8.207				
		6158.1	8.204				
λSi	$\log(Si/H)_*$	λCa	$\log(Ca/H)_*$	λSc	$\log(Sc/H)_*$	λTi	$\log(Ti/H)_*$
5055.984	7.810	5001.479	6.050	4314.083	2.200	4163.644	5.030
5978.930	8.300					4287.873	5.130
6347.110	7.990					4300.042	5.230
						4386.844	5.230
						4394.059	5.040
						4395.051	5.180
						4399.772	4.986
						4417.714	5.490
						4443.801	5.180
λCr	$\log(Cr/H)_*$	λMn	$\log(Mn/H)_*$	λFe	$\log(Fe/H)_*$	λNi	$\log(Ni/H)_*$
4592.049	5.940	4033.062	5.540	4273.326	7.633	4470.472	6.920
4634.070	6.007	4034.483	5.030	4296.570	8.067	4604.982	6.730
4812.337	5.868	4083.628	5.325	4416.830	7.910	5080.528	6.909
5237.329	6.085	4754.042	5.980	4491.405	7.990	5099.927	7.010
5308.440	6.070	4783.427	5.580	4508.288	8.107		
5313.590	6.180			4515.339	8.440		
				4520.224	8.280		
				4522.634	8.054		
				4541.524	7.940		
				4555.890	7.700		
				4666.758	7.510		
λSr	$\log(Sr/H)_*$	λY	$\log(Y/H)_*$	λZr	$\log(Zr/H)_*$		
4077.709	3.990	4883.684	3.246	4149.217	3.820		
4215.520	3.687	4900.120	3.948	4156.240	4.530		
		5087.416	3.170	4208.980	3.770		
				4496.980	3.650		

HD30780							
λC	$\log(C/H)_*$	λO	$\log(O/H)_*$	λNa	$\log(Na/H)_*$	λMg	$\log(Mg/H)_*$
4932.049	8.570	5330.700	8.918	4668.559	6.640	4390.510	8.080
5052.167	8.320	6155.900	8.900	4982.813	6.067	4481.1	8.000
		6158.	8.920				
λSi	$\log(Si/H)_*$	λCa	$\log(Ca/H)_*$	λSc	$\log(Sc/H)_*$	λTi	$\log(Ti/H)_*$
5055.984	7.980	5001.479	6.417	4314.083	3.800	4163.644	4.935
5978.930	8.270	5019.971	6.640	4324.996	3.330	4287.873	5.165
		5285.266	6.650	5031.021	3.123	4300.042	4.710
				5239.813	3.580	4386.844	5.230
						4395.051	5.320
						4399.772	5.360
						4417.714	4.940
λCr	$\log(Cr/H)_*$	λMn	$\log(Mn/H)_*$	λFe	$\log(Fe/H)_*$	λNi	$\log(Ni/H)_*$
4592.049	5.980	4034.483	5.374	4273.326	7.330	4470.472	6.620
4634.070	5.807	4083.628	5.415	4296.570	7.670	4604.982	6.730
4812.337	5.790	4754.042	5.400	4416.830	7.860	5080.528	6.160
5237.329	5.360			4491.405	7.610	5099.927	6.530
5308.440	5.760			4508.288	7.670		
				4515.339	7.670		
				4520.224	7.630		
				4522.634	7.890		
				4541.524	7.720		
λSr	$\log(Sr/H)_*$	λY	$\log(Y/H)_*$	λZr	$\log(Zr/H)_*$		

Table 8. continued.

4077.709	2.570	4883.684	2.570	4149.217	2.510
4215.520	2.700	4900.120	2.585	4156.240	2.990

HD32301

λC	$\log(C/H)_*$	λO	$\log(O/H)_*$	λNa	$\log(Na/H)_*$	λMg	$\log(Mg/H)_*$
4932.049	8.510	5330.700	9.338	4668.559	6.700	4390.510	7.540
5052.167	8.350	6155.900	8.890	4982.813	6.210	4427.994	7.660
5380.337	8.614					4481.1	7.997
5793.120	8.560						
λSi	$\log(Si/H)_*$	λCa	$\log(Ca/H)_*$	λSc	$\log(Sc/H)_*$	λTi	$\log(Ti/H)_*$
5055.984	7.940	5001.479	6.360	4314.083	3.970	4163.644	4.890
5978.930	7.890	5019.971	6.490	4324.996	3.510	4287.873	4.600
6347.110	8.370	5285.266	6.490	5031.021	3.430	4300.042	4.680
				5239.813	2.987	4386.844	5.480
				5526.790	2.930	4395.051	5.476
						4399.772	5.440
λCr	$\log(Cr/H)_*$	λMn	$\log(Mn/H)_*$	λFe	$\log(Fe/H)_*$	λNi	$\log(Ni/H)_*$
4592.049	5.550	4034.483	5.449	4273.326	7.465	4470.472	6.630
4634.070	5.140	4083.628	5.640	4296.570	7.770	4604.982	6.267
4812.337	5.890	4754.042	5.126	4416.830	7.696	5080.528	6.430
5237.329	5.990			4491.405	7.790	5099.927	6.339
5308.440	5.520			4508.288	7.580		
5313.590	5.840			4515.339	7.400		
				4520.224	7.400		
				4522.634	7.459		
				4541.524	7.785		
				4555.890	7.775		
λSr	$\log(Sr/H)_*$	λY	$\log(Y/H)_*$	λZr	$\log(Zr/H)_*$		
4077.709	3.100	4883.684	2.820	4149.217	2.450		
4215.520	2.440	4900.120	2.514	4156.240	2.670		
		5087.416	2.380	4208.980	2.330		

F stars
HD24357

λC	$\log(C/H)_*$	λO	$\log(O/H)_*$	λNa	$\log(Na/H)_*$	λMg	$\log(Mg/H)_*$
		6155-8	8.515	6154.226	6.600	5528.405	7.520
λSi	$\log(Si/H)_*$	λCa	$\log(Ca/H)_*$	λSc	$\log(Sc/H)_*$	λFe	$\log(Fe/H)_*$
				5526.790	3.200	5068.766	7.361
						5072.076	7.363
						5074.748	7.580
						5078.972	7.597
						5506.779	7.330
λNi	$\log(Ni/H)_*$	λY	$\log(Y/H)_*$				
5080.528	6.182						
5084.089	6.209						
5096.854	6.210						

HD25102

λC	$\log(C/H)_*$	λO	$\log(O/H)_*$	λNa	$\log(Na/H)_*$	λMg	$\log(Mg/H)_*$
		6155-8	8.990	6154.226	6.960	5528.405	7.530
				6160.747	6.320		

Table 8. continued.

λSi	$\log(Si/H)_*$	λCa	$\log(Ca/H)_*$	λSc	$\log(Sc/H)_*$	λFe	$\log(Fe/H)_*$
				5526.790	3.005	5068.766	7.270
						5072.076	7.310
						5074.748	7.520
						5078.972	7.340
						5506.779	7.483
λNi	$\log(Ni/H)_*$	λY	$\log(Y/H)_*$				
5080.528	6.290						
5084.089	6.330						

HD26015

λC	$\log(C/H)_*$	λO	$\log(O/H)_*$	λNa	$\log(Na/H)_*$	λMg	$\log(Mg/H)_*$
5052.167	8.710	6155-9	8.780	6154.226	6.400	5528.405	7.428
				6160.747	6.250		
λSi	$\log(Si/H)_*$	λCa	$\log(Ca/H)_*$	λSc	$\log(Sc/H)_*$	λFe	$\log(Fe/H)_*$
5055.984	7.920			5526.790	3.190	5068.766	7.590
						5072.076	7.912
						5074.748	7.560
						5078.972	7.457
						5506.779	7.575
						6136.615	7.680
						6147.835	7.484
						6163.544	7.750
λNi	$\log(Ni/H)_*$	λY	$\log(Y/H)_*$				
5080.528	6.420	5087.416	2.210				
5084.089	6.490						
5096.854	6.430						
5099.927	6.260						

HD26345

λC	$\log(C/H)_*$	λO	$\log(O/H)_*$	λNa	$\log(Na/H)_*$	λMg	$\log(Mg/H)_*$
		6155-8	8.686	6154.226	6.365	5528.405	7.509
				6160.747	6.290		
λSi	$\log(Si/H)_*$	λCa	$\log(Ca/H)_*$	λSc	$\log(Sc/H)_*$	λFe	$\log(Fe/H)_*$
				5526.790	3.120	5068.766	7.499
						5072.076	7.350
						5074.748	7.552
						5078.972	7.570
						5506.779	7.656
λNi	$\log(Ni/H)_*$	λY	$\log(Y/H)_*$				
5080.528	6.270						
5084.089	6.350						

HD26462

λC	$\log(C/H)_*$	λO	$\log(O/H)_*$	λNa	$\log(Na/H)_*$	λMg	$\log(Mg/H)_*$
		6155-8	8.707	6154.226	6.230	5528.405	7.567
				6160.747	6.174		

Table 8. continued.

λSi	$\log(Si/H)_*$	λCa	$\log(Ca/H)_*$	λSc	$\log(Sc/H)_*$	λFe	$\log(Fe/H)_*$
				5526.790	3.145	5068.766	7.400
						5072.076	7.420
						5074.748	7.470
						5078.972	7.596
						5506.779	7.490
						6136.615	7.480
λNi	$\log(Ni/H)_*$	λY	$\log(Y/H)_*$				
5080.528	6.028						
5084.089	6.040						

HD26911

λC	$\log(C/H)_*$	λO	$\log(O/H)_*$	λNa	$\log(Na/H)_*$	λMg	$\log(Mg/H)_*$
5052.167	8.340	6155-8	8.950	6154.226	6.420	5528.405	7.527
				6160.747	6.245		
λSi	$\log(Si/H)_*$	λCa	$\log(Ca/H)_*$	λSc	$\log(Sc/H)_*$	λFe	$\log(Fe/H)_*$
5055.984	7.867	5019.971	6.189	5031.021	3.011	5068.766	7.860
				5526.790	3.151	5072.076	7.408
						5074.748	7.549
						5078.972	7.501
						5506.779	7.580
λNi	$\log(Ni/H)_*$	λY	$\log(Y/H)_*$				
5080.528	6.350	5087.416	2.082				
5084.089	6.270						
5096.854	6.340						
5099.927	6.440						
6163.418	6.590						
6170.567	6.240						
6175.360	6.580						

HD27383

λC	$\log(C/H)_*$	λO	$\log(O/H)_*$	λNa	$\log(Na/H)_*$	λMg	$\log(Mg/H)_*$
		6155-8	8.447	6154.226	6.250	5528.405	7.470
				6160.747	6.301		
λSi	$\log(Si/H)_*$	λCa	$\log(Ca/H)_*$	λSc	$\log(Sc/H)_*$	λFe	$\log(Fe/H)_*$
				5526.790	2.840	5068.766	7.380
						5072.076	7.415
						5074.748	7.537
						5078.972	7.465
						5506.779	7.606
						6136.615	7.850
λNi	$\log(Ni/H)_*$	λY	$\log(Y/H)_*$				
5080.528	6.260						
5084.089	6.600						
5096.854	6.350						

HD27459

λC	$\log(C/H)_*$	λO	$\log(O/H)_*$	λNa	$\log(Na/H)_*$	λMg	$\log(Mg/H)_*$
		6155-8	8.750	6154.226	6.830	5528.405	7.330
				6160.747	6.700		

Table 8. continued.

λSi	$\log(Si/H)_*$	λCa	$\log(Ca/H)_*$	λSc	$\log(Sc/H)_*$	λFe	$\log(Fe/H)_*$
5055.984	7.637			5526.790	3.250	5068.766	7.425
						5072.076	7.740
						5074.748	7.430
						5078.972	7.420
						5506.779	7.510
						6136.615	7.550
						6147.835	7.520
λNi	$\log(Ni/H)_*$	λY	$\log(Y/H)_*$				
5080.528	6.305	5087.416	2.360				
5084.089	6.250						
5096.854	6.090						
5099.927	6.430						
6163.418	6.090						
6170.567	6.420						
HD27524							
λC	$\log(C/H)_*$	λO	$\log(O/H)_*$	λNa	$\log(Na/H)_*$	λMg	$\log(Mg/H)_*$
		6155-8	9.030	6154.226	6.740	5528.405	7.460
				6160.747	6.150		
λSi	$\log(Si/H)_*$	λCa	$\log(Ca/H)_*$	λSc	$\log(Sc/H)_*$	λFe	$\log(Fe/H)_*$
				5526.790	3.160	5068.766	7.448
						5072.076	7.512
						5074.748	7.760
						5078.972	7.280
						5506.779	7.570
λNi	$\log(Ni/H)_*$	λY	$\log(Y/H)_*$				
5080.528	6.420						
5084.089	6.240						
HD27534							
λC	$\log(C/H)_*$	λO	$\log(O/H)_*$	λNa	$\log(Na/H)_*$	λMg	$\log(Mg/H)_*$
		6155-8	9.070	6154.226	6.320	5528.405	7.670
				6160.747	6.270		
λSi	$\log(Si/H)_*$	λCa	$\log(Ca/H)_*$	λSc	$\log(Sc/H)_*$	λFe	$\log(Fe/H)_*$
				5526.790	3.280	5068.766	7.340
						5072.076	7.400
						5074.748	7.607
						5078.972	7.565
						5506.779	7.530
						6136.615	7.525
λNi	$\log(Ni/H)_*$	λY	$\log(Y/H)_*$				
5080.528	5.960						
5084.089	6.539						
HD27561							
λC	$\log(C/H)_*$	λO	$\log(O/H)_*$	λNa	$\log(Na/H)_*$	λMg	$\log(Mg/H)_*$
		6155-8	8.750	6154.226	6.340	5528.405	7.506
				6160.747	6.240		
λSi	$\log(Si/H)_*$	λCa	$\log(Ca/H)_*$	λSc	$\log(Sc/H)_*$	λFe	$\log(Fe/H)_*$
				5526.790	3.030	5068.766	7.410
						5072.076	7.520
						5074.748	7.530
						5078.972	7.570

Table 8. continued.

λ Ni	log(Ni/H) $_{\star}$	λ Y	log(Y/H) $_{\star}$
5080.528	6.110		
5084.089	6.450		
5096.854	6.237		

HD27848

λ C	log(C/H) $_{\star}$	λ O	log(O/H) $_{\star}$	λ Na	log(Na/H) $_{\star}$	λ Mg	log(Mg/H) $_{\star}$
		6155-8	8.730	6154.226	6.245	5528.405	7.604
				6160.747	6.285		
λ Si	log(Si/H) $_{\star}$	λ Ca	log(Ca/H) $_{\star}$	λ Sc	log(Sc/H) $_{\star}$	λ Fe	log(Fe/H) $_{\star}$
				5526.790	3.092	5068.766	7.470
						5072.076	7.430
						5074.748	7.660
						5078.972	7.609
λ Ni	log(Ni/H) $_{\star}$	λ Y	log(Y/H) $_{\star}$				
5080.528	6.310						
5084.089	6.390						

HD27991

λ C	log(C/H) $_{\star}$	λ O	log(O/H) $_{\star}$	λ Na	log(Na/H) $_{\star}$	λ Mg	log(Mg/H) $_{\star}$
		6155-8	8.388	6154.226	6.400	5528.405	7.453
				6160.747	6.370		
λ Si	log(Si/H) $_{\star}$	λ Ca	log(Ca/H) $_{\star}$	λ Sc	log(Sc/H) $_{\star}$	λ Fe	log(Fe/H) $_{\star}$
				5526.790	3.170	5068.766	7.463
						5072.076	7.460
						5074.748	7.510
						5078.972	7.690
λ Ni	log(Ni/H) $_{\star}$	λ Y	log(Y/H) $_{\star}$				
5080.528	6.260						
5084.089	6.170						

HD28363

λ C	log(C/H) $_{\star}$	λ O	log(O/H) $_{\star}$	λ Na	log(Na/H) $_{\star}$	λ Mg	log(Mg/H) $_{\star}$
		6155-8	8.450	6154.226	6.439		
				6160.747	6.430		
λ Si	log(Si/H) $_{\star}$	λ Ca	log(Ca/H) $_{\star}$	λ Sc	log(Sc/H) $_{\star}$	λ Fe	log(Fe/H) $_{\star}$
						5068.766	7.420
						5072.076	7.360
						5074.748	7.529
						5078.972	7.570
						5506.779	7.470
						6136.615	7.510
λ Ni	log(Ni/H) $_{\star}$	λ Y	log(Y/H) $_{\star}$				
5080.528	6.027						
5084.089	6.350						

HD28406

λ C	log(C/H) $_{\star}$	λ O	log(O/H) $_{\star}$	λ Na	log(Na/H) $_{\star}$	λ Mg	log(Mg/H) $_{\star}$
5052.167	8.310	6155-8	8.570	6154.226	6.330	5528.405	7.527
				6160.747	6.230		

Table 8. continued.

λSi	$\log(Si/H)_*$	λCa	$\log(Ca/H)_*$	λSc	$\log(Sc/H)_*$	λFe	$\log(Fe/H)_*$
5055.984	7.900	5019.971	6.590	5031.021	2.970	5068.766	7.499
		5021.138	6.257	5526.790	3.062	5072.076	7.800
						5074.748	7.390
						5078.972	7.410
						5506.779	7.580
						6136.615	7.700
						6147.835	7.499
						6163.544	7.509
λNi	$\log(Ni/H)_*$	λY	$\log(Y/H)_*$				
5080.528	6.440	5087.416	2.088				
5084.089	6.170						
5096.854	6.420						
5099.927	6.135						
6163.418	6.297						

HD28556

λC	$\log(C/H)_*$	λO	$\log(O/H)_*$	λNa	$\log(Na/H)_*$	λMg	$\log(Mg/H)_*$
		6155-8	8.710			5528.405	7.620
λSi	$\log(Si/H)_*$	λCa	$\log(Ca/H)_*$	λSc	$\log(Sc/H)_*$	λFe	$\log(Fe/H)_*$
				5526.790	3.200	5068.766	7.390
						5072.076	7.400
						5074.748	7.690
						5078.972	7.618
						5506.779	7.502
λNi	$\log(Ni/H)_*$	λY	$\log(Y/H)_*$				
5080.528	6.174						
5084.089	6.380						

HD28568

λC	$\log(C/H)_*$	λO	$\log(O/H)_*$	λNa	$\log(Na/H)_*$	λMg	$\log(Mg/H)_*$
		6155-8	8.970	6154.226	6.800	5528.405	7.583
				6160.747	6.317		
λSi	$\log(Si/H)_*$	λCa	$\log(Ca/H)_*$	λSc	$\log(Sc/H)_*$	λFe	$\log(Fe/H)_*$
				5526.790	3.145	5068.766	7.390
						5072.076	7.449
						5074.748	7.545
						5078.972	7.350
						5506.779	7.490
						6136.615	7.570
λNi	$\log(Ni/H)_*$	λY	$\log(Y/H)_*$				
5080.528	6.490						
5084.089	5.940						
5096.854	6.298						

HD28677

λC	$\log(C/H)_*$	λO	$\log(O/H)_*$	λNa	$\log(Na/H)_*$	λMg	$\log(Mg/H)_*$
		6155-8	8.797			5528.405	7.880

Table 8. continued.

λSi	$\log(Si/H)_*$	λCa	$\log(Ca/H)_*$	λSc	$\log(Sc/H)_*$	λFe	$\log(Fe/H)_*$
				5526.790	3.660	5068.766	7.394
						5072.076	7.350
						5074.748	7.659
						5078.972	7.641
λNi	$\log(Ni/H)_*$	λY	$\log(Y/H)_*$				
5080.528	6.203						
5084.089	6.320						
HD28736							
λC	$\log(C/H)_*$	λO	$\log(O/H)_*$	λNa	$\log(Na/H)_*$	λMg	$\log(Mg/H)_*$
		6155-8	9.070	6160.747	6.230	5528.405	7.630
λSi	$\log(Si/H)_*$	λCa	$\log(Ca/H)_*$	λSc	$\log(Sc/H)_*$	λFe	$\log(Fe/H)_*$
				5031.021	3.200	5068.766	7.280
						5072.076	7.435
						5074.748	7.560
						5078.972	7.535
						5506.779	7.536
λNi	$\log(Ni/H)_*$	λY	$\log(Y/H)_*$				
5080.528	6.260						
5084.089	6.330						
HD28911							
λC	$\log(C/H)_*$	λO	$\log(O/H)_*$	λNa	$\log(Na/H)_*$	λMg	$\log(Mg/H)_*$
		6155-8	9.050	6154.226	6.750	5528.405	7.583
				6160.747	6.255		
λSi	$\log(Si/H)_*$	λCa	$\log(Ca/H)_*$	λSc	$\log(Sc/H)_*$	λFe	$\log(Fe/H)_*$
				5526.790	3.160	5068.766	7.436
						5072.076	7.398
						5074.748	7.570
						5078.972	7.700
						5506.779	7.460
						6136.615	7.456
λNi	$\log(Ni/H)_*$	λY	$\log(Y/H)_*$				
5080.528	6.219						
5084.089	6.340						
5096.854	6.330						
HD29169							
λC	$\log(C/H)_*$	λO	$\log(O/H)_*$	λNa	$\log(Na/H)_*$	λMg	$\log(Mg/H)_*$
		6155-8	8.968	6154.226	6.700	5528.405	7.609
				6160.747	6.800		
λSi	$\log(Si/H)_*$	λCa	$\log(Ca/H)_*$	λSc	$\log(Sc/H)_*$	λFe	$\log(Fe/H)_*$
				5526.790	3.290	5068.766	7.328
						5072.076	7.503
						5074.748	7.620
						5078.972	7.600
						5506.779	7.350
λNi	$\log(Ni/H)_*$	λY	$\log(Y/H)_*$				
5080.528	6.120						
5084.089	6.260						

Table 8. continued.

HD29225							
λC	$\log(C/H)_\star$	λO	$\log(O/H)_\star$	λNa	$\log(Na/H)_\star$	λMg	$\log(Mg/H)_\star$
5052.167	8.290	6155-8	8.985	6154.226	6.700		
				6160.747	6.216		
λSi	$\log(Si/H)_\star$	λCa	$\log(Ca/H)_\star$	λSc	$\log(Sc/H)_\star$	λFe	$\log(Fe/H)_\star$
5055.984	8.010	5019.971	6.313	5526.790	2.920	5068.766	7.462
						5072.076	7.610
						5074.748	7.520
						5078.972	7.630
						5506.779	7.600
λNi	$\log(Ni/H)_\star$	λY	$\log(Y/H)_\star$				
5080.528	6.460	5087.416	2.110				
5084.089	6.500						
5096.854	6.310						
5099.927	6.440						
6163.418	6.480						

HD30034							
λC	$\log(C/H)_\star$	λO	$\log(O/H)_\star$	λNa	$\log(Na/H)_\star$	λMg	$\log(Mg/H)_\star$
		6155-8	8.640	6154.226	6.780	5528.405	7.860
				6160.747	6.800		
λSi	$\log(Si/H)_\star$	λCa	$\log(Ca/H)_\star$	λSc	$\log(Sc/H)_\star$	λFe	$\log(Fe/H)_\star$
				5526.790	3.541	5068.766	7.380
						5072.076	7.486
						5074.748	7.800
						5078.972	7.600
						5506.779	7.420
λNi	$\log(Ni/H)_\star$	λY	$\log(Y/H)_\star$				
6154.226	6.780						
6160.747	6.800						

HD30810							
λC	$\log(C/H)_\star$	λO	$\log(O/H)_\star$	λNa	$\log(Na/H)_\star$	λMg	$\log(Mg/H)_\star$
		6155-8	8.730	6154.226	6.320		
				6160.747	6.340		
λSi	$\log(Si/H)_\star$	λCa	$\log(Ca/H)_\star$	λSc	$\log(Sc/H)_\star$	λFe	$\log(Fe/H)_\star$
						5068.766	7.320
						5072.076	7.490
						5074.748	7.520
						5078.972	7.445
λNi	$\log(Ni/H)_\star$	λY	$\log(Y/H)_\star$				
5080.528	6.164						
5084.089	6.260						

HD30869							
λC	$\log(C/H)_\star$	λO	$\log(O/H)_\star$	λNa	$\log(Na/H)_\star$	λMg	$\log(Mg/H)_\star$
		6155-8	8.790	6154.226	6.380		
				6160.747	6.190		
λSi	$\log(Si/H)_\star$	λCa	$\log(Ca/H)_\star$	λSc	$\log(Sc/H)_\star$	λFe	$\log(Fe/H)_\star$
						5068.766	7.400
						5072.076	7.360
						5074.748	7.600
						5078.972	7.410

Table 8. continued.

λ Ni	$\log(\text{Ni}/\text{H})_{\star}$	λ Y	$\log(\text{Y}/\text{H})_{\star}$
5080.528	6.040		
5084.089	6.250		
HD31236			
λ C	$\log(\text{C}/\text{H})_{\star}$	λ O	$\log(\text{O}/\text{H})_{\star}$
		6155-8	8.752
			6154.226
			6160.747
			6.380
			6.080
λ Si	$\log(\text{Si}/\text{H})_{\star}$	λ Ca	$\log(\text{Ca}/\text{H})_{\star}$
			5526.790
			3.300
			5068.766
			5072.076
			5074.748
			5078.972
			7.132
			7.505
			7.660
			7.437
λ Ni	$\log(\text{Ni}/\text{H})_{\star}$	λ Y	$\log(\text{Y}/\text{H})_{\star}$
5080.528	6.321		
HD31845			
λ C	$\log(\text{C}/\text{H})_{\star}$	λ O	$\log(\text{O}/\text{H})_{\star}$
		6155-8	8.550
			6154.226
			6160.747
			6.206
			6.250
λ Si	$\log(\text{Si}/\text{H})_{\star}$	λ Ca	$\log(\text{Ca}/\text{H})_{\star}$
			5526.790
			2.910
			5068.766
			5072.076
			5074.748
			5078.972
			5506.779
			6136.615
			7.526
			7.490
			7.540
			7.640
			7.690
			7.640
λ Ni	$\log(\text{Ni}/\text{H})_{\star}$	λ Y	$\log(\text{Y}/\text{H})_{\star}$
5080.528	6.480		
5084.089	6.320		
HD18404			
λ C	$\log(\text{C}/\text{H})_{\star}$	λ O	$\log(\text{O}/\text{H})_{\star}$
5052.167	8.280	6155-8	8.379
			6154.226
			6160.747
			6.098
			6.330
λ Si	$\log(\text{Si}/\text{H})_{\star}$	λ Ca	$\log(\text{Ca}/\text{H})_{\star}$
5055.984	7.487	5019.971	6.840
			5031.021
			5526.790
			2.860
			3.059
			5068.766
			5072.076
			5074.748
			5078.972
			5506.779
			6136.615
			6147.835
			6163.544
			6173.336
			6187.990
			7.444
			7.490
			7.740
			7.706
			7.585
			7.496
			7.444
			7.490
			7.679
			7.550
			7.703

Table 8. continued.

λ Ni	log(Ni/H) $_{\star}$	λ Y	log(Y/H) $_{\star}$								
5080.528	6.480	5087.416	2.108								
5084.089	6.220										
5096.854	5.931										
5099.927	6.270										
6163.418	6.280										
6170.567	6.453										
6175.360	6.295										
Procyon											
λ C	log(C/H) $_{\star}$	λ O	log(O/H) $_{\star}$	λ Na	log(Na/H) $_{\star}$	λ Mg	log(Mg/H) $_{\star}$				
4932.049	8.320	6155.961	8.800	4668.559	6.440	4390.510	7.479				
5052.167	8.530	6158.149	8.600	4982.813	6.080	4427.994	7.545				
5380.337	8.440						4481.0				
λ Si	log(Si/H) $_{\star}$	λ Ca	log(Ca/H) $_{\star}$	λ Sc	log(Sc/H) $_{\star}$	λ Ti	log(Ti/H) $_{\star}$				
5055.984	7.600	4472.050	6.300	4314.083	3.290	4163.644	5.001				
5978.930	7.550	5001.479	6.320	4324.996	3.150	4287.873	5.100				
6347.110	7.680	5021.138	6.100	5031.021	3.250	4300.042	5.004				
λ Cr	log(Cr/H) $_{\star}$	λ Mn	log(Mn/H) $_{\star}$	λ Fe	log(Fe/H) $_{\star}$	λ Ni	log(Ni/H) $_{\star}$				
4592.049	5.500	4033.062	5.450	4273.326	7.370	4470.472	5.720				
4616.629	5.492	4034.483	5.440	4416.830	7.460	4604.982	6.200				
4634.070	5.600	4055.544	5.510	4491.405	7.480	5080.528	6.180				
4812.337	5.690	4083.628	5.400	4508.288	7.500	5099.927	6.110				
5237.329	5.500						5476.904				
5308.440	5.570						5476.904				
5313.590	5.500						5476.904				
λ Sr	log(Sr/H) $_{\star}$	λ Y	log(Y/H) $_{\star}$	λ Zr	log(Zr/H) $_{\star}$						
4077.709	3.120	4883.684	2.420	4149.217	2.560						
4215.520	3.240	4900.120	2.100	4156.240	2.840						
		5087.416	2.380	4161.210	2.800						
		5200.406	2.300	4208.980	2.600						
				4496.980	2.750						